

SURFACE WATER – GROUNDWATER INTERACTION AND WATER QUALITY OF THE GUADALUPE RIVER BASIN AND THE TRINITY AQUIFER IN WESTERN COMAL COUNTY, TEXAS

2019 GEO 377K/391K
Applied Karst Hydrogeology

Project Report
December 9, 2019



PREFACE

As a hydrogeologist at the Edwards Aquifer Authority (EAA) and adjunct faculty at The University of Texas at Austin, Jackson School of Geoscience (UT), I have integrated current research objectives of the EAA with the field geology course at UT, “Applied Karst Hydrogeology.” This class has been offered every year since 2011, and each class becomes more directly involved with EAA investigations of the Edwards and Trinity aquifers. In the fall of 2019, the Karst Hydro class addressed the research topic of surface water and groundwater interaction on the Guadalupe River near Honey Creek Cave, the longest cave in Texas. The class learned contemporary theories in karst science, practical skills in field hydrogeology, and how to integrate theory and practice to test hypotheses in the real world. Using techniques of stream gauging, geochemical sampling, and groundwater level mapping, the 2019 class performed a series of investigations to understand how the Guadalupe River and its associated tributaries interact with the underlying Trinity Aquifer, and help determine background aquifer conditions in an area expected to experience rapid growth in the near future. While the class study results do not completely solve the mysteries of this complex system, they do shed new light on our understanding of the river-aquifer dynamics.

Dr. Marcus Gary

Field Operations Project Manager, Edwards Aquifer Authority

Adjunct Assistant Professor, The University of Texas at Austin, Jackson School of Geosciences



TABLE OF CONTENTS

PREFACE	2
ABSTRACT	6
TABLE OF CONTENTS	
List of Figures.....	7
List of Tables.....	8
List of Appendices.....	9
CHAPTER 1 – Introduction	10
Problem Statement.....	10
Background.....	10
Project Area and Description.....	10
Surface water hydrology.....	12
Geologic framework: faults and caves.....	12
Hydrogeologic setting.....	15
Past work on recharge in the study area.....	16
Overview of methods used in study	16
CHAPTER 2 – Hydrogeologic Framework and Major Features	18
Introduction.....	18
Esser’s Fault.....	19
Discovery and Background.....	19
Methods.....	20
Results.....	21
Rebecca Spring.....	22
Background.....	22
Methods.....	22
Results.....	23
Discussion.....	24
Esser’s Fault.....	24
Rebecca Cave.....	24
CHAPTER 3 – Surface Water Flows	25
Introduction.....	25
Guadalupe River basin.....	25
Stream gauging sites.....	26
References.....	26
Hypothesis.....	26
Methods.....	26
Site selection.....	26
Stream gauging with FlowTrackers.....	27

Stream gauging with ADCP.....	29
Supplemental data.....	30
Results.....	32
Discussion.....	38
Recharge and discharge.....	38
Gain/loss survey.....	38
Conclusion.....	38
CHAPTER 4 – Groundwater	39
Background.....	39
Hydrostratigraphy and geologic framework.....	39
Well locations.....	41
Methods and data.....	43
Manual well measurements.....	43
Additional water level measurements.....	45
Hydrostratigraphic unit determination.....	45
Potentiometric surface map.....	45
Hydrographs.....	45
Drawdown curve.....	46
Results.....	46
Potentiometric surface map.....	46
Hydrographs.....	49
Drawdown curve.....	50
Discussion.....	51
Potentiometric surface map.....	51
Hydrographs.....	53
Drawdown curve.....	54
Conclusion.....	54
CHAPTER 5 – Water Quality	55
Background.....	55
Methods.....	56
Sample collection.....	56
Analytical methods.....	60
Major ions.....	60
Results.....	64
Major ions.....	64
Nutrients.....	64
Isotopes.....	66
PFAAS and PPCP.....	67

Discussion.....	70
Major ions.....	70
Nutrients.....	71
Isotopes.....	72
PFAAS and PPCP.....	72
Conclusion.....	72
CHAPTER 6 – Conclusion.....	74
CHAPTER 7- References.....	75
CHAPTER 8 –Appendices.....	79

ABSTRACT

As Central Texas and the hill country continue to experience rapid population growth, the need for potable water supply and wastewater solutions intensifies. The primary source of potable water in the area is groundwater, with over 2 million people relying on the Edwards and Trinity Aquifers for municipal and industrial water use. Yet the Middle Trinity Aquifer in this region has been listed as a “critical water supply area” since 1989, and modeling efforts have demonstrated possible groundwater depletion by 2050 from pumping alone (Mace, 2000; Texas Groundwater Protection Unit, 1989). The complex karstic nature of this region and the spatial and temporal variability of groundwater and surface water interaction make estimates of recharge and contamination risk difficult. Therefore, this report seeks to characterize the current conditions of the Guadalupe River basin and Middle Trinity Aquifer in the vicinity of Honey Creek in western Comal County to provide a comparative baseline as population, pumping, and wastewater discharge into the study area increase in the coming years. This report details data collected by the Applied Karst Hydrogeology Fall 2019 course at the University of Texas at Austin, taught by Dr. Marcus Gary. Reported findings include a map of Rebecca Cave, stream flow measurements from 19 sites, gain/loss estimates for a section of the Guadalupe River, groundwater elevation levels from 23 wells, an estimated potentiometric map of the Middle Trinity aquifer in the study area, and a suite of water chemistry analyses from wells and streams at 10 sites. The major conclusions of this study are that this region has surface water – groundwater connectivity, especially due to the large karst features such as Honey Creek Cave, and that the major ion concentrations in the water samples are highly controlled by the dominant lithology, with the Lower Trinity Aquifer having high concentrations of chlorine, sulfate, sodium, and potassium, the Middle Trinity Aquifer and the surface water having high concentrations of calcium and bicarbonate. These results provide a characterization of the Honey Creek study area during a time period of Fall 2019 and with hope, will be utilized for future studies and hydrogeological characterizations of the hill country and Central Texas region.

LIST OF FIGURES

CHAPTER 1

Fig 1.0: A map of study area within the Honey Creek State Natural Area

Fig 1.1: A map of sample sites near Honey Creek Cave

Fig 1.2: The Karst19 team in Honey Creek Cave just before Whistler's Mother

Fig 1.3: A drawing map of Honey Creek Cave up to Whistler's Mother

Fig 1.4: Stratigraphic column of the study area

CHAPTER 2

Fig 2.0: Karst19 team preparing to enter Honey Creek Cave.

Fig 2.1: Historical marker at Esser's Crossing

Fig 2.2: Overview image of the outcrop where Esser's Fault was found and mapped.

Fig 2.3: An image and stereonet of Esser's Fault

Fig 2.4: An image of Chance Bolduc emerging from Rebecca Creek.

Fig 2.5: A hand-drawn map of Rebecca Cave.

Fig 2.6: An image of Chance Bolduc entering Rebecca Cave.

CHAPTER 3

Fig 3.0: Map of the Guadalupe River Basin (Ockerman and Slattery, 2008)

Fig 3.1: Karst19 team using FlowTrackers at the Guadalupe River.

Fig 3.2: FlowTracker and FlowTracker 2 (SonTek, 2007)

Fig 3.3: FlowTracker probe in orientation relative to the streamflow (SonTek, 2007)

Fig 3.4: Karst19 using FlowTracker at Rebecca Springs.

Fig 3.5: Karst19 team using ADCP to measure flow on the Guadalupe River.

Fig 3.6: The ADCP attached to the end of a kayak below Miller Falls.

Fig 3.7: USGS Gauge at the Guadalupe River near Spring Branch, TX discharge.

Fig 3.8: USGS Gauge at the Guadalupe River near Berghelm, TX discharge.

Fig 3.9: Gain/loss survey results for Guadalupe River, July 2019.

Fig 3.10: Gain/loss survey results for Guadalupe River, August 2019.

Fig 3.11: Gain/loss survey results for Guadalupe River, September 2019.

Fig 3.12: Gain/loss survey results for Guadalupe River, November 2019.

CHAPTER 4

Fig 4.0: Hydrostratigraphic units for Comal and Bexar Counties (Clark et al., 2016)

Fig 4.1: Locations of the 23 wells with water level data

Fig 4.2: Image of Leica RTK receiver and tripod

Fig 4.3: Image of E-line and sonic meter

Fig 4.4: Potentiometric surface map of Middle-Trinity Aquifer within the Honey Creek Study Area

Fig 4.5: Map of Lower Trinity Aquifer well sites with well elevations.

Fig 4.6: Map of Middle Trinity Aquifer well sites that were used for hydrograph analysis

Fig 4.7: Map of Lower Trinity Aquifer well site that was used for hydrograph analysis

Fig 4.8: Drawdown curve of well site 68-13-102

Fig 4.9: Potentiometric surface map of Hill Country Trinity Portion of the Middle-Zone of the Trinity Aquifer (Toll et al., 2018)

CHAPTER 5

Fig 5.0: Students inserting e-line into well to measure depth to water.

Fig 5.1: Well pump and generator on truck.

Fig 5.2: Pump inserted into well after the decontamination process.

Fig 5.3: Eureka Manta 30 probe

Fig 5.4: A water sample sent to chemical analysis laboratory.

Fig 5.5: Organizing the sample containers

Fig 5.6: Samples being taken and organized from well.

Fig 5.7: Piper diagram illustrating the major ions concentrations in the study area

Fig 5.8: Water type based on major ions classification, using the Piper diagram.

Fig 5.9: The nitrate as N concentration across all ten sites.

Fig 5.10: D/H and O18/O16 across all ten sites.

Fig 5.11: pMC and D13C across all ten sites.

Fig 5.12: The concentration of the PFASs at all the river sites.

Fig 5.13: Geologic map and schematic stratigraphic column in the study area.

LIST OF TABLES

CHAPTER 3

Table 3.0: Summary of total discharge for the study, July-November 2019.

Table 3.1: Summary data table for all discharge data collected in study.

CHAPTER 4

Table 4.0: Well site information in the Honey Creek Study Area.

CHAPTER 5

Table 5.0: Stations where water quality samples were collected

Table 5.1: Data used to build the Piper plot reported by TestAmerica Laboratories.

Table 5.2: Values of Valence and Atomic weight used to calculate ion concentrations in meq/L

Table 5.3: Ions concentrations in meq/L

Table 5.4: Ion concentrations normalized to the total ions' concentration.

Table 5.5: The results of the lab PFAS analysis for all the sites and key.

Table 5.6: The PCPPs tested for in the water samples.

LIST OF APPENDICES

CHAPTER 3-Surface water

CHAPTER 4-Groundwater

CHAPTER 5-Water Chemistry

CHAPTER 1 – Introduction

PROBLEM STATEMENT

To characterize baseline hydrologic and water quality conditions of the Guadalupe River basin in western Comal County, Texas, and to identify areas of possible surface water – groundwater interaction.

BACKGROUND

PROJECT AREA DESCRIPTION

This study focuses on the area of Honey Creek and the surrounding Guadalupe River basin near the city of Spring Branch, Texas (Fig 1.0). This area is just northwest of the Balcones Escarpment, which forms the edge of the Edwards Plateau. 40% of Texas' total population lives along the Balcones Escarpment in cities such as Waco, Austin, San Marcos, and San Antonio (Texas Dept. of Transportation, 2016). The study area is about 30 miles north of San Antonio, which is Texas' 2nd largest city by population and one of the fastest growing cities in the nation (World Population Review.com, 2019). The study takes place in an area commonly referred to as the "Hill Country," the region on top of the Edwards Plateau, which is characterized by rivers, hills, and springs sprinkled across an oak juniper forest and sporadic grassland. Historically the Hill Country has been occupied by small, unincorporated towns and rural agricultural settlements. Recently, however, population in the Hill Country has boomed alongside the growth of the major cities surrounding it. This increase in population has brought with it an increased demand for neighborhood subdivisions, wastewater treatment plants, and water supply (Hill Country Alliance, 2008).

According to Texas Parks and Wildlife, around 60% of the total Hill Country water demand is met by surface water (TPW, accessed 2019). At least 2 million people in this area rely primarily on groundwater, however, as demonstrated by the Texas Water Development Board's growing record of groundwater wells, which currently includes over 140,000 wells from 2001 which are responsible for approximately 6.95 million acre-feet of pumped groundwater in 2015 alone (TWDB, GWDB, accessed 2019). Many Hill Country streams also gain or lose water along their course from groundwater contribution through springs and sinkholes. As climate models predict decreased precipitation in this region while population projections continue to grow, a complete understanding of the interactions between groundwater and surface water in this area is essential for resource conservation.

SURFACE WATER HYDROLOGY

The Guadalupe River basin extends directly across the Hill Country and is effectively parallel to several other major rivers such as the Colorado, Blanco, and Brazos Rivers. These rivers cross Texas from the northwest heading southeast towards the Gulf of Mexico. Many of these rivers are dammed multiple times for the purpose of creating reservoirs for water storage and for flood control and recreation. The study area for this report is upstream of Canyon Lake, the nearest artificial reservoir formed from the dammed Guadalupe River. At least five springs, collectively named Wolle Springs, were documented at this location before the flooding of the lake in 1964. The discharge record for these springs is 15 cfs. in 1944 and 22 cfs. in 1955 (Brune, 1975; Brune, 1981).

The Guadalupe River in this area receives significant portions of its baseflow from tributaries, many of which originate from springs. Several of these springs and tributaries are investigated in this report, including Honey Creek and Honey Creek Cave Spring, Rebecca Creek and Rebecca Springs, and Spring Branch Creek. Magic Springs, the origination of Spring Branch Creek, was not directly observed in this study, but provides flow to Spring Branch Creek. Magic Springs, which emerges from the Glen Rose Limestone, also has a cave, which had been explored for 100 meters by the 1980s. This cave, like Rebecca Cave, was also the site of a well (Brune, 1981).

The data for this report was collected during the fall of 2019 after a summer of relatively little rain. Small portions of Texas were beginning to enter “severe” or “exceptional” drought conditions as defined by the National Integrated Drought Information System, although there was no formal drought in this area at the time of the study (NIDIS, 2019). The most recent major drought in Texas lasted for five years from 2011 to 2015. Its severity did not exceed the drought of record, however, which lasted for seven years in the 1950s and resulted in the creation of the Texas Water Development Board (TWDB, 2019).

GEOLOGIC FRAMEWORK: FAULTS AND CAVES

In addition to focusing on the surface and groundwater interaction between Honey Creek, the Guadalupe River, and the Middle Trinity Aquifer, this study also focuses on the influence of Honey Creek Cave and Honey Creek on the Guadalupe River. Honey Creek Cave was formally discovered in 1943 and is the longest cave in Texas with a current mapped extent of 21 miles (Fig 1.1). It is still not fully mapped, as current expeditions to uncharted areas require intensive scuba expertise as well as long stretches of hauling gear through dry portions of the cave. The cave is home to numerous species such as the aquatic Comal and Honey Creek Cave blind salamanders and the Cave Myotis Bat. Honey Creek Cave essentially functions as a large underground river whose final discharge point is not yet known. Only three entrances are currently mapped, including the dry and wet entrance near the Honey Creek State Natural Area and one additional artificial shaft created in 1985 to facilitate exploration deeper into the cave (Menking, 2019).

As part of this study, the Karst19 team took a field trip into Honey Creek Cave and swam to the landmark of Whistler’s Mother from the dry entrance near the State Natural Area (Fig 1.2; Fig 1.3). They also visited and mapped Rebecca Cave. In addition to cave studies, this project also reports the dip angle for a newly discovered fault on the Guadalupe River, which is now named Esser’s Fault.

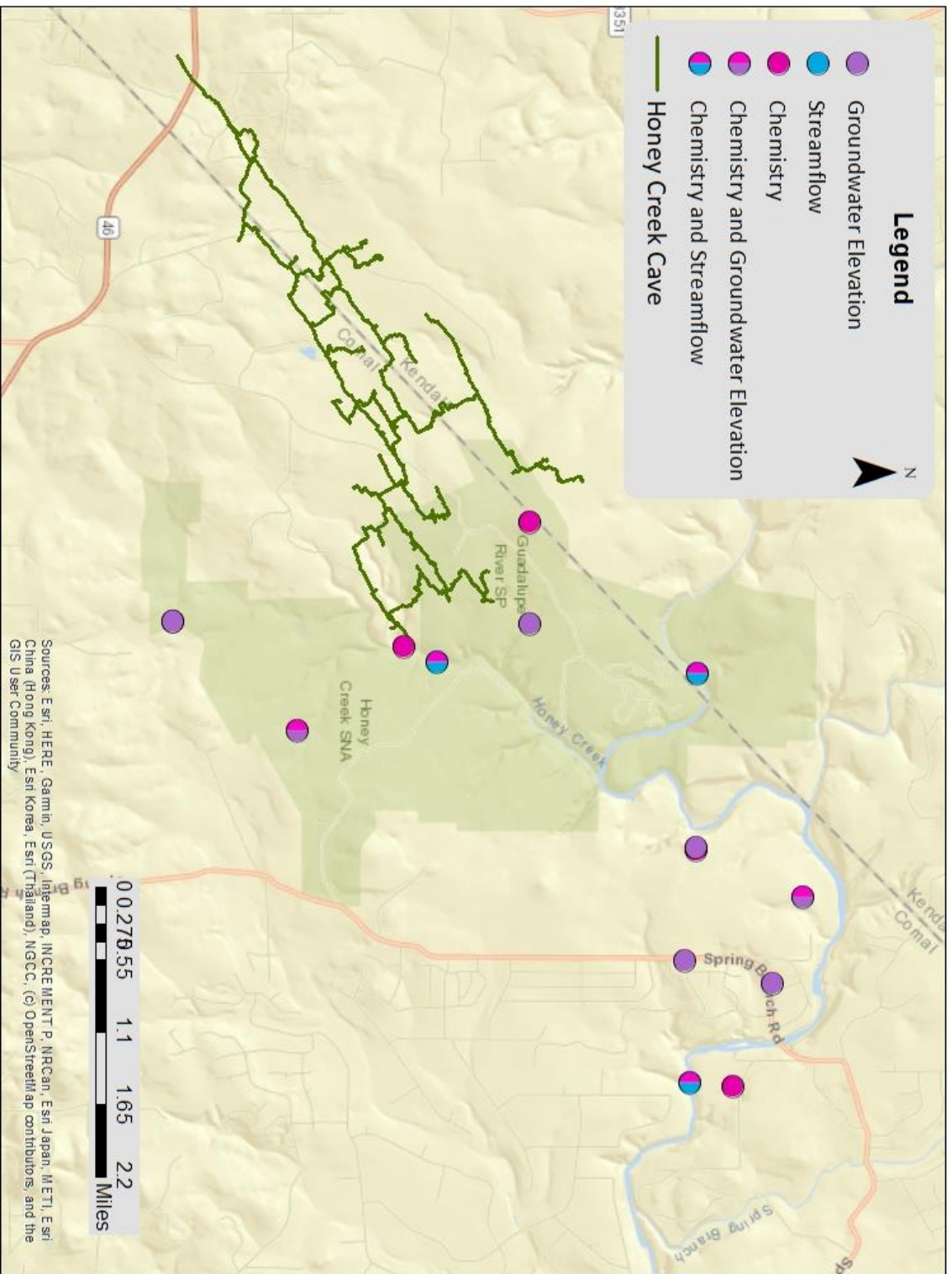


Figure 1.1 Map of sample sites near Honey Creek Cave. Map of cave from Menking, 2019.



Figure 1.2: A picture of the class in front of Whistler's Mother in Honey Creek Cave. The class swam from the dry entrance of Honey Creek Cave to Whistler's Mother and back

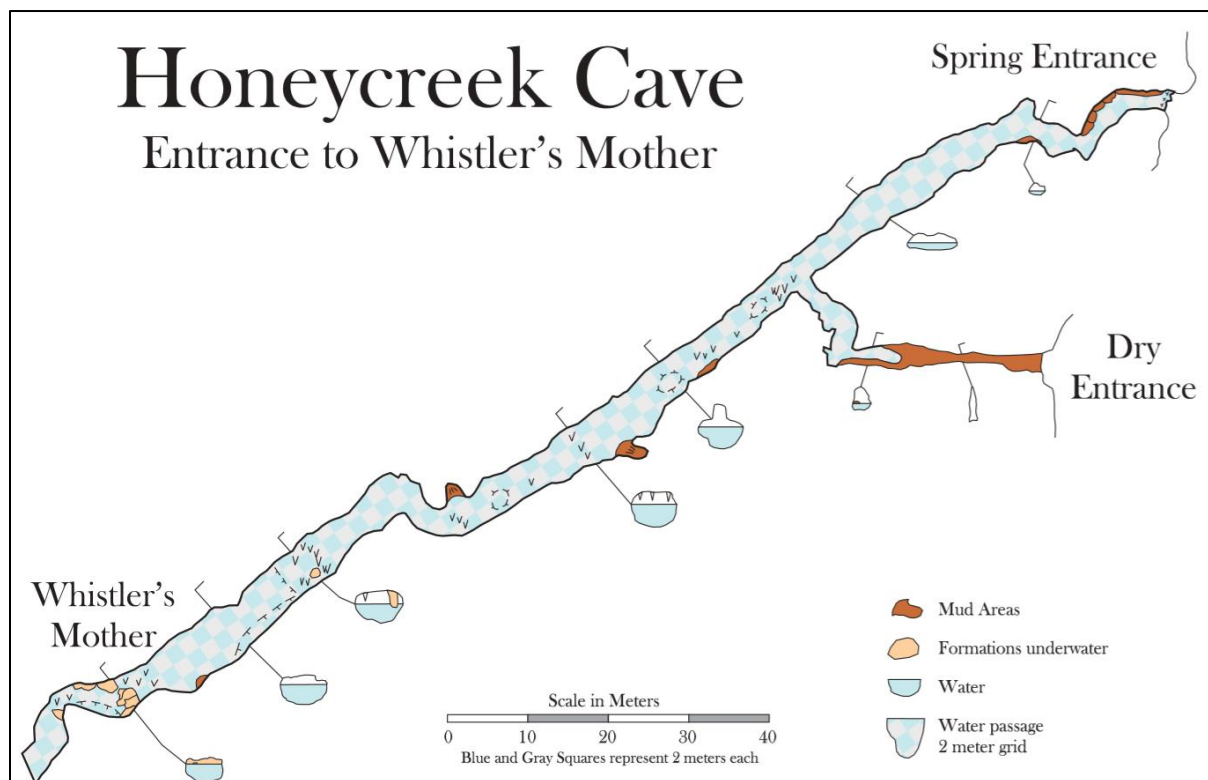


Figure 1.3: Map of the first section of Honey Creek Cave (Menking, 2019).

HYDROGEOLOGIC SETTING

The primary aquifers in this region are the Lower Trinity, Middle Trinity, Upper Trinity, and Edwards Aquifers (Fig 1.4) All of the units which comprise these aquifers were formed during the early Cretaceous when this area was characterized by a shallow marine-shelf environment (Clark, 2003). The Middle Trinity Aquifer is the focus of this report, however a brief overview of the larger hydrogeologic setting is provided here for context.

Era	System	Group	Stratigraphic unit		Hydrologic unit	
Cenozoic	Quaternary		Alluvium		Alluvium	
Mesozoic	Cretaceous	Edwards	Segovia Formation		Edwards Group	
			Fort Terrett Formation			
		Trinity	Glen Rose Limestone	Upper Member	Trinity Aquifer System	Upper Trinity
				Lower Member		Middle Trinity
			Hensell Sand/Bexar Shale			
			Cow Creek Limestone			
			Hammett Shale			Confining unit
			Sligo Formation			Lower Trinity
Sycamore Sand/Hosston Formation						
Paleozoic		Undifferentiated Pre-Cretaceous rock				

Figure 1.4: A stratigraphic column of the study area (TWDB, 2011)

The Lower Trinity Aquifer includes the Sligo and Hosston formations. Several wells in this report extend into the Lower Trinity. It is becoming an increasingly utilized resource for water as the Middle Trinity begins to show signs of overexploitation. The Lower Trinity has historically been avoided by well owners due to its high load of dissolved solids compared to the Middle Trinity; however, it is now being drilled more frequently (Veni, 1994).

The Middle Trinity, the focus of this report, is composed of the Lower Glen Rose Limestone, the Hensell Sand, and the Cow Creek Limestone. The Middle Trinity Aquifer is primarily unconfined in this region, except where the Upper Glen Rose is present, at which point it begins to act increasingly confined. The Middle Trinity Aquifer overlies the Hammett Shale, which also serves as a confining unit between the Lower and Middle Trinity aquifers. The Lower Glen Rose Limestone of the Middle Trinity is one of the most cavernous units in the area and is the stratigraphic location of Honey Creek Cave (Veni, 1994).

The Upper Trinity Aquifer exists in only one stratigraphic unit, the Upper Glen Rose Limestone. This unit is mostly devoid of caves as a result of its interbedded clay and marl layers which block

the infiltration of water and slow the dissolution necessary for cave formation. The exception to this lack of caves occurs in eastern Comal County and Northern Bexar County, outside of the study area, where caves like Natural Bridge Caverns exist along the edge of the Upper Glen Rose. Because of the clay and marl beds, the Upper Trinity aquifer can also be thought of as a semi-permeable confining unit for the Edwards. In addition to clay and marl, the Upper Trinity also has zones with high levels of gypsum, which make it a rare location for wells (Veni, 1994).

The Edwards Aquifer, sometimes labeled the Edwards Balcones Fault Zone Aquifer, is divided into four geographic segments: the San Antonio Segment, the Barton Springs Segment, the Northern Balcones Segment, and the Washita Prairie Segment. The San Antonio segment is the nearest to the study area. This segment was once briefly named the “Edwards Underground River” by the Texas Water Commission in 1992 as an attempt to encourage the legislature to view it more like surface water for regulatory purposes. The name did not hold, however, and was quickly overturned (Veni, 1994; TWC, 1992).

Water quality differs between all of the aquifer units. In some locations, the Trinity aquifers have been found to have higher total dissolved solids but lower concentrations of nitrogen than the Edwards (Fahlquist and Ardist, 2004). This difference in nitrogen could be linked to the larger degree of urbanization over the Edwards. Water quality analysis by the USGS has also shown that all of these aquifers are comprised of relatively young water, as demonstrated by the presence of tritium, which was first released in great quantities in the atmosphere during the nuclear tests of the 1940s and 50s. The presence of this compound in the water indicates that the groundwater was in contact with the atmosphere in the last fifty years (Fahlquist and Ardist, 2004).

PAST WORK ON RECHARGE IN THE STUDY AREA

Constraining recharge to groundwater systems in the Texas hill country requires understanding of two categories of interconnected flow: groundwater flow between the Trinity and Edwards aquifers and groundwater-surface water interaction within aquifers individually. Groundwater-surface water interaction can occur within a single aquifer as well as in locations where surface water crosses exposed portions of multiple aquifers. Studies which focus on groundwater-surface water interaction are of increasing interest to water resource management stakeholders and scientists and include recent publications such as Martin, 2019; Mahler, 2011a; Mahler, 2011b; Gary, 2013; and Hunt, 2017. These studies are essential for resource management as the extent of groundwater-surface water interaction has impacts on recharge prediction, contaminant transport, and long term regional drawdown. Additionally, many groundwater regulation stipulations in Texas use spring flow at key springs such as Jacobs Well, Pleasant Valley Springs, and Barton Springs as triggers for pumping reductions.

OVERVIEW OF METHODS USED IN STUDY

The term karst originated in modern day southeast Europe as a description of a rocky, human deforested landscape (Gams, 1991). Modern definitions of karst rely not on the quality of the surface terrain, but on the presence of dissolution conduits and fluid circulation in the subsurface (Klimchouk, 2015). Karstification occurs when water infiltrates soils, gains acidity, and dissolves calcium carbonate rock, resulting in the expansion of preferential flow paths and the creation of

conduits, including caves. This dissolution causes karst to have 'triple porosity' made up of its matrix, fracture, and conduit components. It also necessitates a specific toolset for evaluating karst, as described by White (2002). This study utilizes several of the karst characterization techniques listed by White, including water budget analysis through stream flow surveys, cave exploration, water quality analysis, and a wise use of test wells (White, 2002).

The work presented in this report includes original data collected by the Applied Karst Hydrogeology course of 2019, taught by Dr. Marcus Gary of the Edwards Aquifer Authority, data from the Texas Water Development Board Well Database, from the USGS stream gauge network, and from previously published work. Significant assistance was provided by the Edwards Aquifer Authority and the Comal Trinity Groundwater Conservation District.

CHAPTER 2 – Hydrogeologic Framework and Major Features

INTRODUCTION

This chapter focuses on the mapping of Esser's Fault and Rebecca Cave. The two resulting maps indicate the importance of faulting and karst caves on the hydrology of the area. They also highlight the importance of structural features on dictating the extent of groundwater – surface water interaction.

The products from this chapter include:

- A stereonet of Esser's Fault dip angle.
- A map of Rebecca Cave surveyed and created for this report.

A further discussion of the surface water hydrology of Rebecca Creek and Rebecca Springs, both of which originate in Rebecca Cave, can be found in Chapter 3.



Figure 2.0: The Karst19 team preparing to enter Honey Creek Cave.

ESSER'S FAULT

DISCOVERY AND BACKGROUND

While camping near the Guadalupe River (site GUAD230), the class observed faulting at a cliff outcrop and recorded the strikes and dips of the accessible fault planes. This fault was previously unrecorded, so the class searched for a fitting name. Thankfully, this section of the Guadalupe River has been important to Texan settlers for many years and is the site of "Esser's Crossing," a wagon path and river crossing which was first established in the 1800s (Fig 2.1). This crossing informed the current site of the Guadalupe River bridge on FM 311, very near to the camping site for the class on Mr. Larry Hull's land.



Figure 2.1: An image of the historical marker at Esser's Crossing. The plaque is located near the FM 311 bridge that crosses over the Guadalupe River. It details the significance of the area for travelers in the 1800's.

Faulting in the rest of the study area is dominated by the Balcones Fault Zone (BFZ), which strikes dominantly northeast and exhibits gradual curvature in an eastern direction on its northeast side until it strikes almost completely to the east. Individual faults associated with the BFZ are nearly vertical and can demonstrate nearly 300 to 400 meters of displacement (Barker, 1994).

METHODS

The phone apps RockD and Stereonet Mobile were used to measure the strike and dip of Esser's Fault and to plot the results as a stereonet. Each strike and dip was taken as a set of three repetitions on the most planar surface available. The measurement locations were chosen because of their clear offset horizontal bedding planes where all of the rocks seemed in place.



Figure 2.2: An overview image of the outcrop where Esser's Fault was found and mapped.

RESULTS

Fig 2.3 shows a close-up image and a stereonet of Esser's Fault. The fault has an average strike of 298° and a dip of 62° . The strike angle is nearly perpendicular to the faulting in the Balcones Fault Zone. The fault also runs perpendicularly through the Guadalupe River and is vertically perpendicular to the cliff outcrop where it was observed.

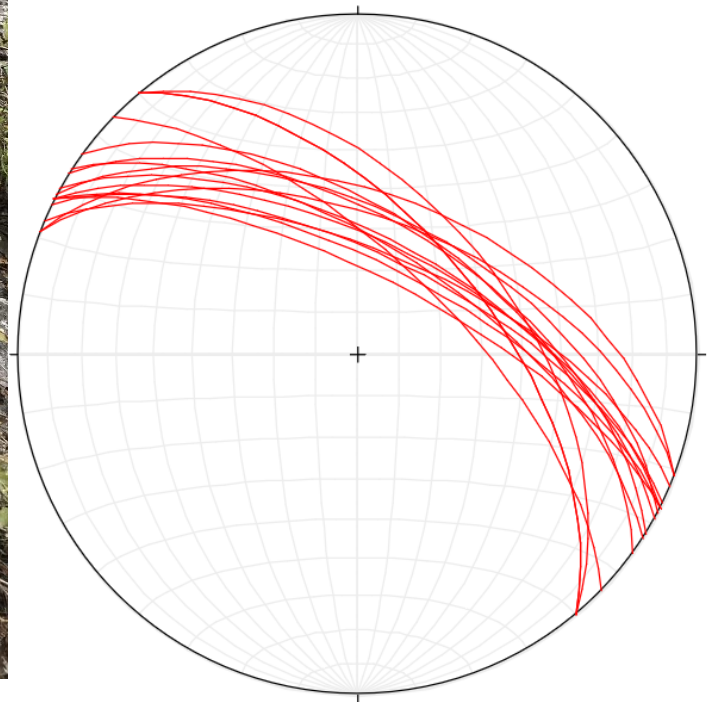
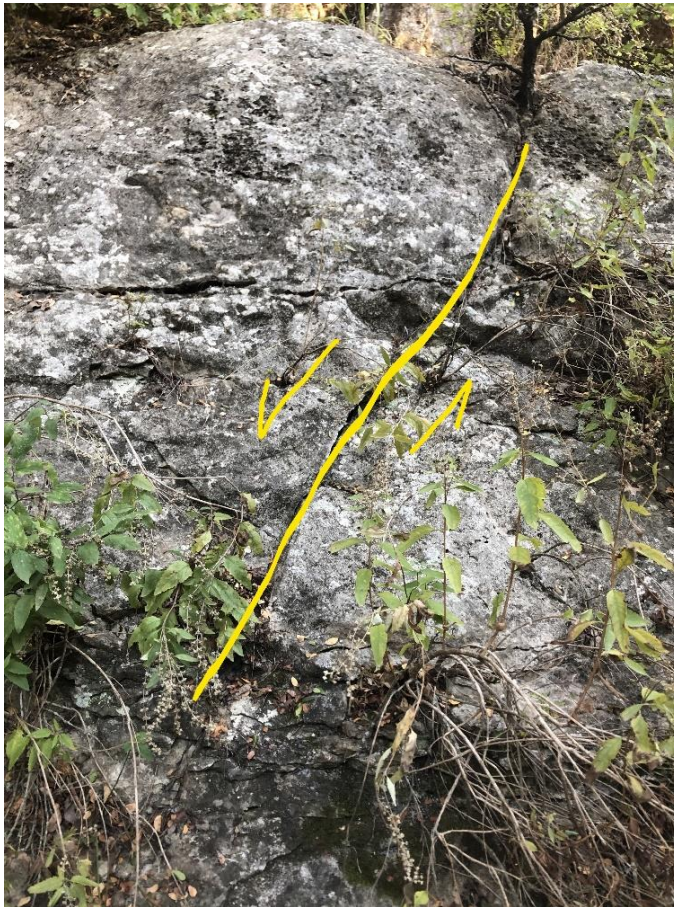


Figure 2.3: (Left) a close-up image of Esser's Fault. (Right) A stereonet made in Stereonet showing fault plane measurements from Esser's Crossing.

REBECCA SPRING

BACKGROUND

Rebecca Cave and Rebecca Springs emerge from the Cow Creek Limestone. A supply well once penetrated the cave but was removed within the past few decades. Just outside the cave entrance a small concrete dam holds the spring water to fill a small reservoir before the water overflows to a channel, which connects the creek. Modern and historical flow measurements from Rebecca Springs and this artificial reservoir are reported and discussed in Chapter 3.

METHODS

Rebecca Cave was mapped using a tape measure and a SUUTO. Seven stations were created with individual measurements of inclination, declination, distance between the stations, and the estimated distance to the top, bottom, left, and right of the cave extent. Using this data, a map was drawn of the cave and filled in with sketched details such as observed water flow, the location of the old well, and rock piles within the cave. The dam and channel infrastructure outside of the cave will be reported in Chapter 3.



Fig 2.4: Chance Bolduc emerging from Rebecca Creek after a successful mapping expedition.

RESULTS

Figure 2.5 shows the map of Rebecca Cave. The distance from the cave entrance to the spring is about 17 feet. The cave has an average floor to ceiling height of about two feet and an average water depth of about four inches. The width of the cave at the mouth is seven feet and the cave remains this width for the first 12 feet. After this depth, the cave opens up into a larger room where the spring, the old well casing, and two other passages are located. The two observed passages were inaccessible because of low ceilings and rocks.

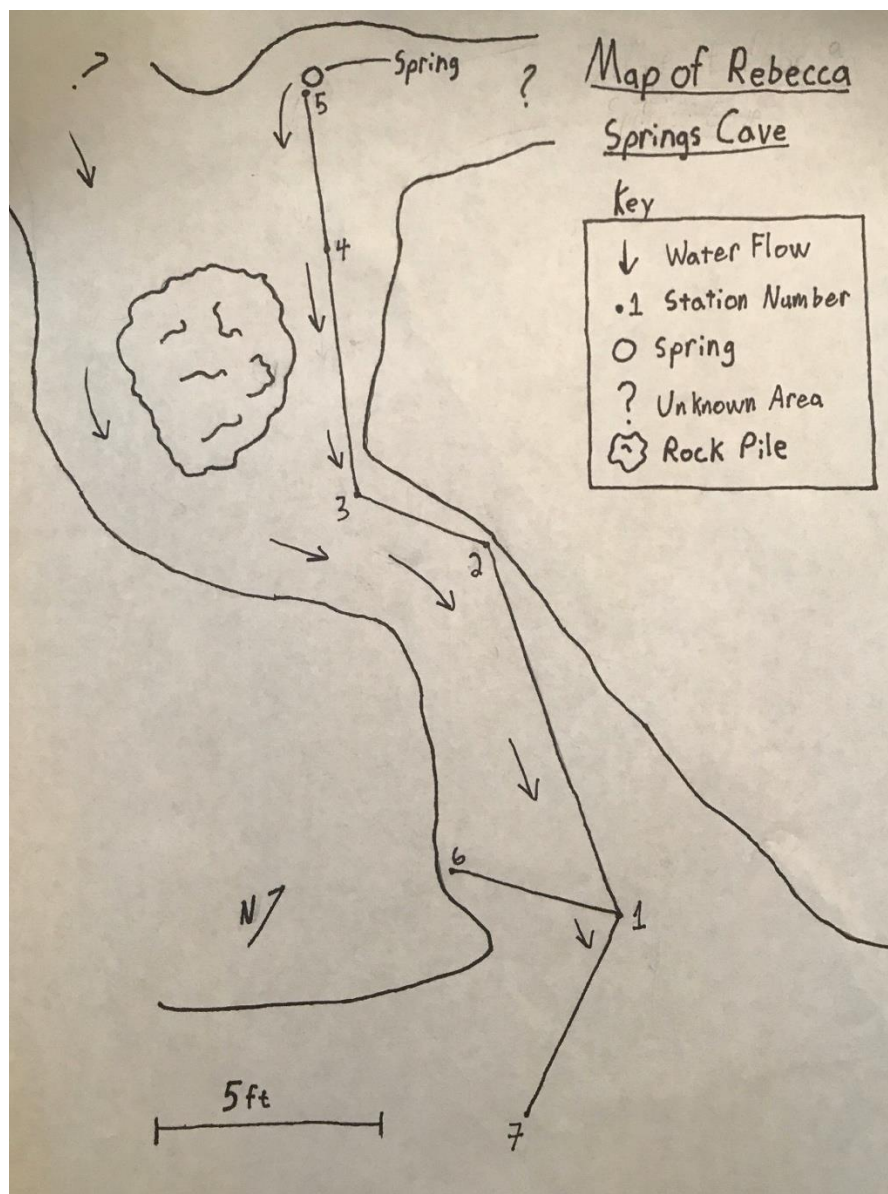


Fig 2.5: A map of Rebecca Cave

DISCUSSION

ESSER'S FAULT

The presence of faulting in this area is not surprising given the Balcones Fault Zone in the region. However, even small faults such as Esser's Fault can facilitate surface water – groundwater interaction. Faults such as this may play a role in the Guadalupe River either gaining or losing at different points along its reach and during different hydrologic conditions.

REBECCA CAVE

Although Rebecca Cave has a much smaller volume than Honey Creek Cave, it still demonstrates the importance of karstification and conduits in the interplay between groundwater and surface water in the area. This cave is also a good example of how karst features can create opportunities for groundwater extraction. The well that previously sat on the top of the slope above Rebecca Springs Cave is now removed, however its casing was still visible from within the cave. The well served as a supply well for the settlement around Rebecca Creek and was extremely productive, probably because it was tapping the cave spring.



Fig 2.6: Chance Bolduc entering Rebecca Cave.

CHAPTER 3 – Surface Water

INTRODUCTION

GUADALUPE RIVER BASIN

The Guadalupe River's headwaters begin in southwestern Kerr County, located northwest of San Antonio. The river is about 400 miles long and its drainage area is about 10,000 square miles with over half a million citizens reside in the basin. The Guadalupe's main tributaries are the Blanco River and San Marcos River, and its major springs in the basin include Comal Springs, San Marcos Springs, and Hueco Springs. The climate of the basin is subtropical and sub-humid, meaning that the region experiences hot summers and mild winters. Floods and droughts are also common, as the region experiences varying amounts of precipitation (Ockerman and Slattery, 2008).

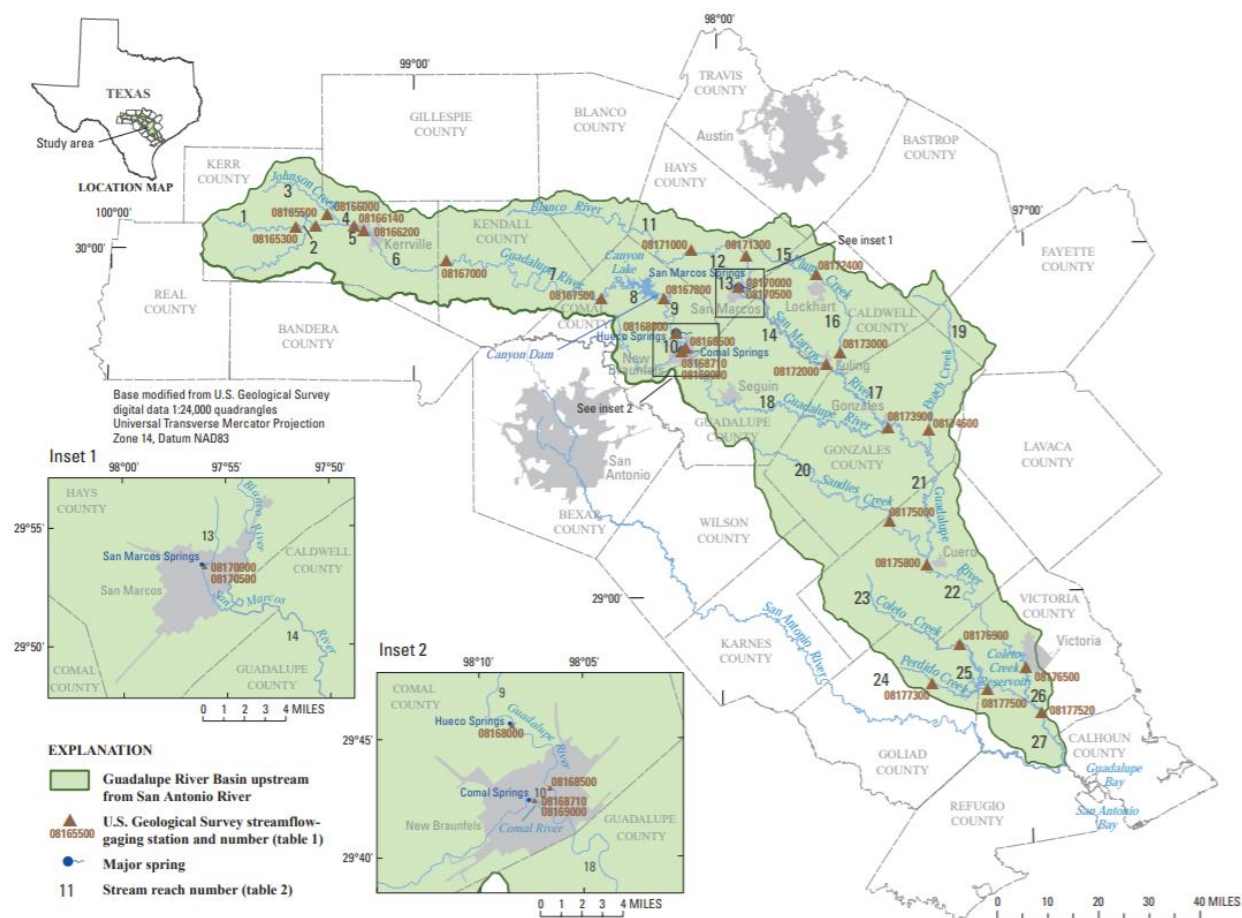


Figure 1. Guadalupe River Basin, south-central Texas, locations of U.S. Geological Survey streamflow-gaging stations, and locations of stream reaches used for analysis of streamflow conditions.

Figure 3.0: Map of the Guadalupe River Basin (Ockerman and Slattery, 2008)

STREAM GAUGING SITES

Our class went to several rivers, creeks, streams, and springs throughout the Guadalupe River Basin in western Comal County throughout the study. The Guadalupe River is located next to our campsite at Larry Hull's ranch, which also hosts the USGS FM311 gauge used in our supplemental data. We took several ADV (Sontek Flowtracker) and ADCP (Sontek M9) measurements at multiple locations along this reach of the river. Several members of the Karst 2019 class swam through Honey Creek Cave to observe the karst conduit network of the Middle Trinity Aquifer in this area. ADV measurements were taken in the Guadalupe River, Spring Branch Creek, Honey Creek and at several other locations. At Rebecca Springs, we performed a cave survey and mapped its tributaries. Honey Creek Cave Spring is located next to Honey Creek Cave, the longest cave in Texas. Little Honey Creek Cave Spring is a narrow spring located near Honey Creek Cave. We have data for Magic Spring by measuring the flow at Spring Branch Creek downstream of Magic Spring, because as a class we did not visit this spring.

REFERENCES

We used the following sources to help us better understand the Guadalupe River Basin and the equipment we used. Ockerman and Slattery (2008) describes the Guadalupe River Basin. The SonTek manual (SonTek 2007) provided two images and information on how FlowTrackers work. Turnipseed and Sauer's USGS report (2010) presented us with information on the functionality of ADVs and ADCPs.

HYPOTHESIS

We hypothesize that there is significant recharge within the Guadalupe River Basin along major faults within the channel, as well as major input from karst springs in the watershed.

METHODS

SITE SELECTION

The sites utilized for discharge measurement transects are located in the Guadalupe River Basin, within the river or contributing creeks, springs, and tributaries. The sites were chosen based on regions of hypothesized recharge from faulting and known spring discharge. Many of the sites were focused near Miller Falls, the largest hypothesized recharge region. From these measurements, we compiled a data table to quantify spring contribution and gain/loss maps to map the regions of recharge into the aquifer. This data will better characterize the recharge and groundwater-surface water interactions. At each site, the cross-sections were selected on accessibility, water depth, and limited channel obstructions. For quality data collection there must be no major obstructions in the channel during measurement, such as large boulders, heavy vegetation or debris (Turnipseed and Sauer, 2010). For FlowTracker measurements, it was also important that the water depth was preferably 1.5 feet or less. In Figure 3.1 Karst19 Team is using the FlowTrackers to measure at GUAD230, which is an ideal cross-section as described above.



Fig. 3.1 Karst19 Team using FlowTrackers to stream gauge at the FM 311 bridge in the Guadalupe River. Duplicate measurements were taken at this site to ensure accuracy of results and to compare to USGS gauge measurements at this site.

STREAM GAUGING WITH FLOWTRACKERS

The discharge measurements were collected with a SonTek FlowTracker, FlowTracker2, and an ADCP (Fig. 3.3 & 3.6). Both models of FlowTracker are handheld Acoustic Doppler Velocimeters (ADV), where an acoustic signal is emitted, traveling through the sample volume (water volume between acoustic receivers Fig. 3.3), and is reflected in all directions by particles suspended in the water column. The acoustic signal reflects off the particles, where a Doppler shift occurs in the acoustic frequency, and then the phase change can be measured. This technique assumes the particle and water velocity are equivalent. After a selection of the measurements site, each transect was cleared of any obstructions such as large rocks and vegetation. The measuring tape (slack-line) was oriented perpendicular to the flow in the channel and was tightly tied down to either side of the channel. The measuring tape was used to measure the width of the channel and to divide the channel into evenly spaced measurement intervals. The tape also allowed for each measurement to be accurately angled perpendicular to the flow (Turnipseed and Sauer, 2010), (SonTek 2007).



Fig 3.2 FlowTracker and FlowTracker2, respectively (SonTek, 2007)

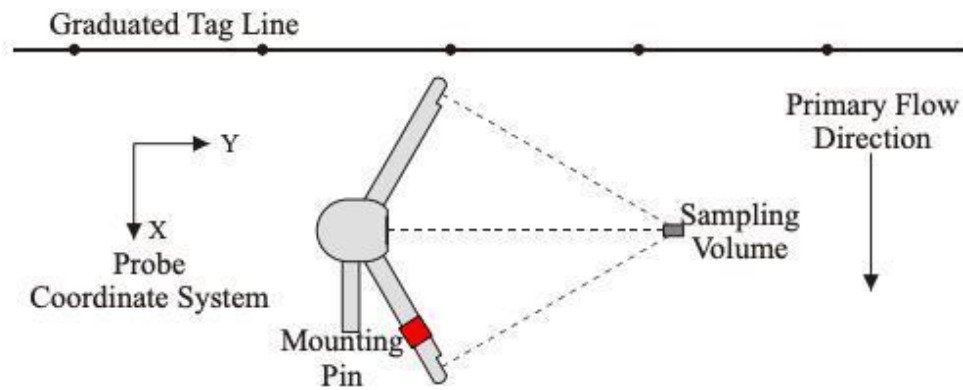


Fig. 3.3 FlowTracker probe in orientation relative to the stream flow (SonTek)

Many of the sites within our study were spring flow locations. At a spring site, the channels are much narrower and sometimes require more unique measurements, as shown below. The FlowTracker requires at least 10 measurement points across a channel, so at spring sites measurements were taken about every 0.2 feet. These spring channels were an important part of our study because they are contributing to the baseflow in the larger streams and the Guadalupe River, therefore it was important to capture their flow contribution.



Fig. 3.4 Karst19 Team using FlowTracker to measure the spring flow at a weir at Rebecca Springs Cave to understand contribution to Rebecca Spring Creek

STREAM GAUGING WITH ADCP

ADCP is an acronym for Acoustic Doppler Current Profiler. We used an ADCP in boat-form by mounting it to the front of a kayak and paddling across the rivers perpendicular to flow (Fig. 3.6). The ADCP's also use the Doppler shift to measure changes in velocity magnitude and direction. Acoustic pulses were sent out by the instrument, bounced off of sediment, and then reflected back to the ADCP. A computer was used to capture data results in real-time from the ADCP. ADCP's divide streams into about 20 to 30 different sections and measure velocity through each column of water. However, ADCP's cannot measure velocity near a river's surface or stream beds (Turnipseed and Sauer, 2010).



Fig. 3.5 Karst19 Team using the ADCP to measure flow of the Guadalupe River at Larry Hull's campsite.



Fig. 3.6 The ADCP is attached to the end of a kayak and was used to measure the flow above and below Miller Falls to quantify recharge to

SUPPLEMENTAL DATA

Data collected by the FlowTrackers and ADCPs were supplemented by external data from the USGS gauging stations. We can further discuss our results in comparison to the USGS gauges that fall within our study area. The two gauges within our study region were Guadalupe River at Spring Branch, TX (Guad230) and Guadalupe River at FM 474, both of which are to the west of Canyon Lake and upstream of Miller Falls. The USGS gauge 'Guadalupe River at Spring Branch, TX' (Guad230) shows accurate and comparable flow to those recorded in our summary data tables. We can see that discharge decreased gradually over the end of summer as did our flow measurements as the study progressed. We can also see that there was a major storm pulse in late August before the class data was collected (Fig. 3.7).

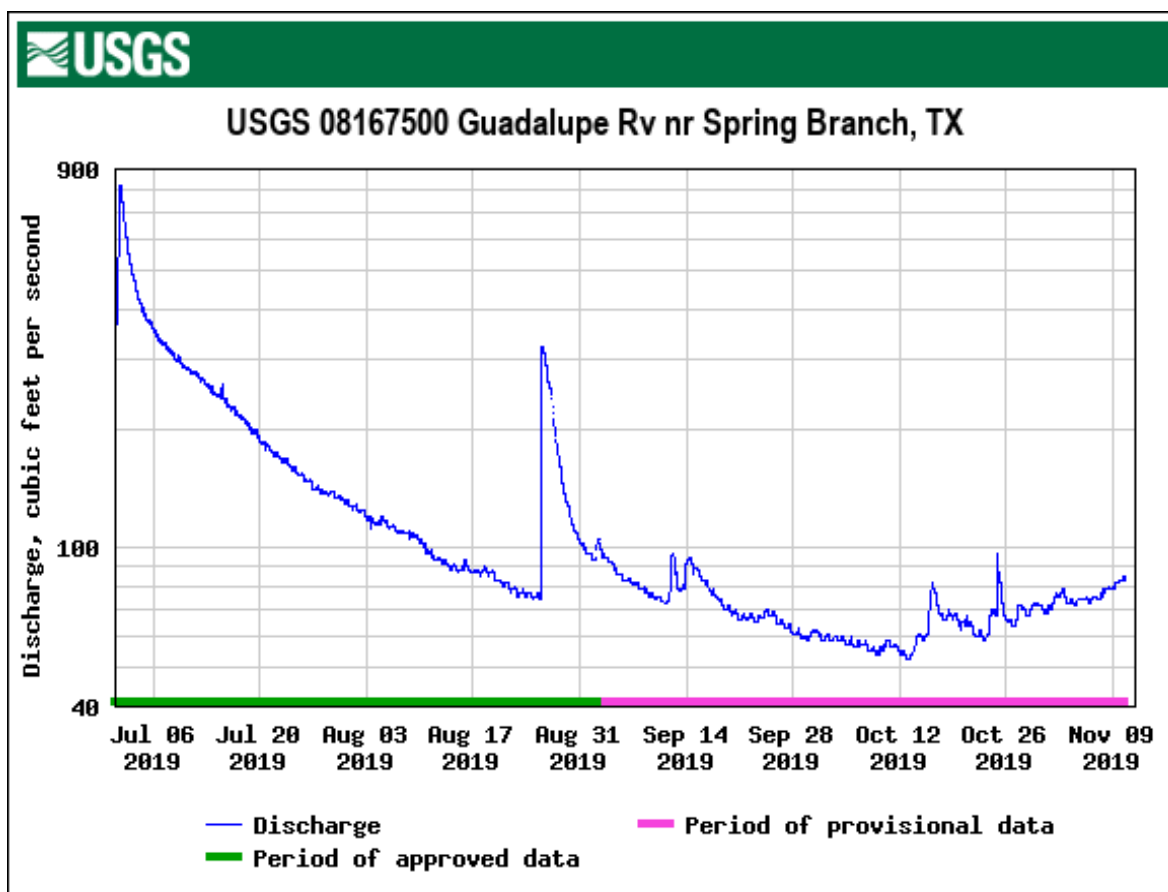


Fig. 3.7 USGS Gauge - Guadalupe River, Spring Branch, TX

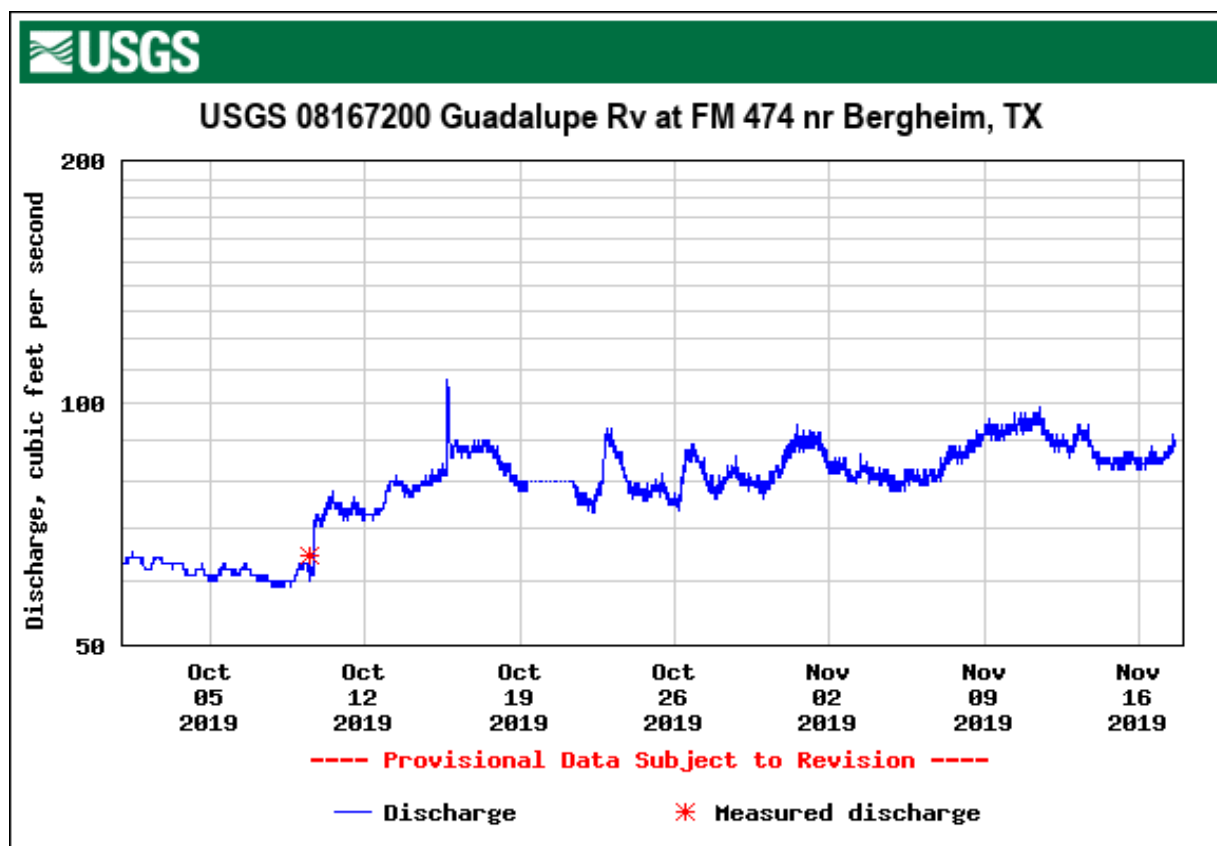


Fig. 3.8 USGS Gauge – Guadalupe River at FM 474 Bergheim, TX

Further upstream is the FM 474 USGS Gauging station, shown in Fig 3.8. This gauge is a more recent installment and only has discharge data dating back to October 1st 2019, while the Spring Branch gauge dates back before the beginning of the study. If we compare the data after October 1st we see very similar discharge and simultaneous peaks at both gauges. Both gauges are upstream of Miller Falls, where we hypothesized the greatest recharge occurs. This makes sense that the gauges have similar discharge because the major recharge features are downstream of both, rather than between.

RESULTS

The results of our study include a summary discharge table, estimated total recharge to the aquifer, and mapped regions of recharge.

NAME	Date	Operator	Instrument	Discharge (cfs)
SW Guad200	9/28/19	Karst19	Flowtracker 1	65.021
Little Honey Creek Spring	9/28/19	Karst19	Flowtracker	2.038
Guad 212	9/29/19	Karst19	Flowtracker 1	68.253
GUAD230	9/14/19	Karst19	Flowtracker 2	92.1873
GUAD230	9/14/19	Karst19	Flowtracker 1	126.8259
GUADP 2.2	9/28/19		Flowtracker 1	65.0208
Guad 237	9/14/19	Karst19	ADCP	95.32
GUAD230	9/14/19	Karst19	ADCP	100.711
GUAD239	9/14/19	Karst19	ADCP	87.289
N/A	9/28/19	Karst19	Flowtracker 1	2.0388
Guad230	9/14/19	Karst19	ADCP	96.964
8167500		EAA		141
GUAD229	7/29/19	EAA	ADP	152.13
GUAD230	7/29/19	EAA	ADP	142.575
GUAD235	7/29/19	EAA	ADP	148.638
GUAD240	7/29/19	EAA	ADP	132.631

GUAD250	7/29/19	EAA	ADP	115.728
8167800	7/29/19	EAA	Gage	198
8168500	7/29/19	EAA	Gage	282
GUAD240	7/29/19	EAA	ADP	61.157
GUAD245	8/23/19	EAA	ADP	48.843
GUAD250	8/23/19	EAA	ADP	46.86
8167500	8/23/19	EAA	Gage	77.1
8167800	8/23/19	EAA	Gage	142
8168500	8/23/19	EAA	Gage	214
GUAD250	11/4/19	KARST19	FlowTracker	46.7117
RPS001	10/20/19	KARST19	FlowTracker	0.4808
RSP002	10/20/19	KARST19	FlowTracker	0.2999
N/A	11/2/19	KARST19	FlowTracker	2.1483
HONC010	9/28/19	KARST19	FlowTracker	2.0388

Table 3.0 Summary Data Table for all discharge data collected on springs, creeks and the Guadalupe River.

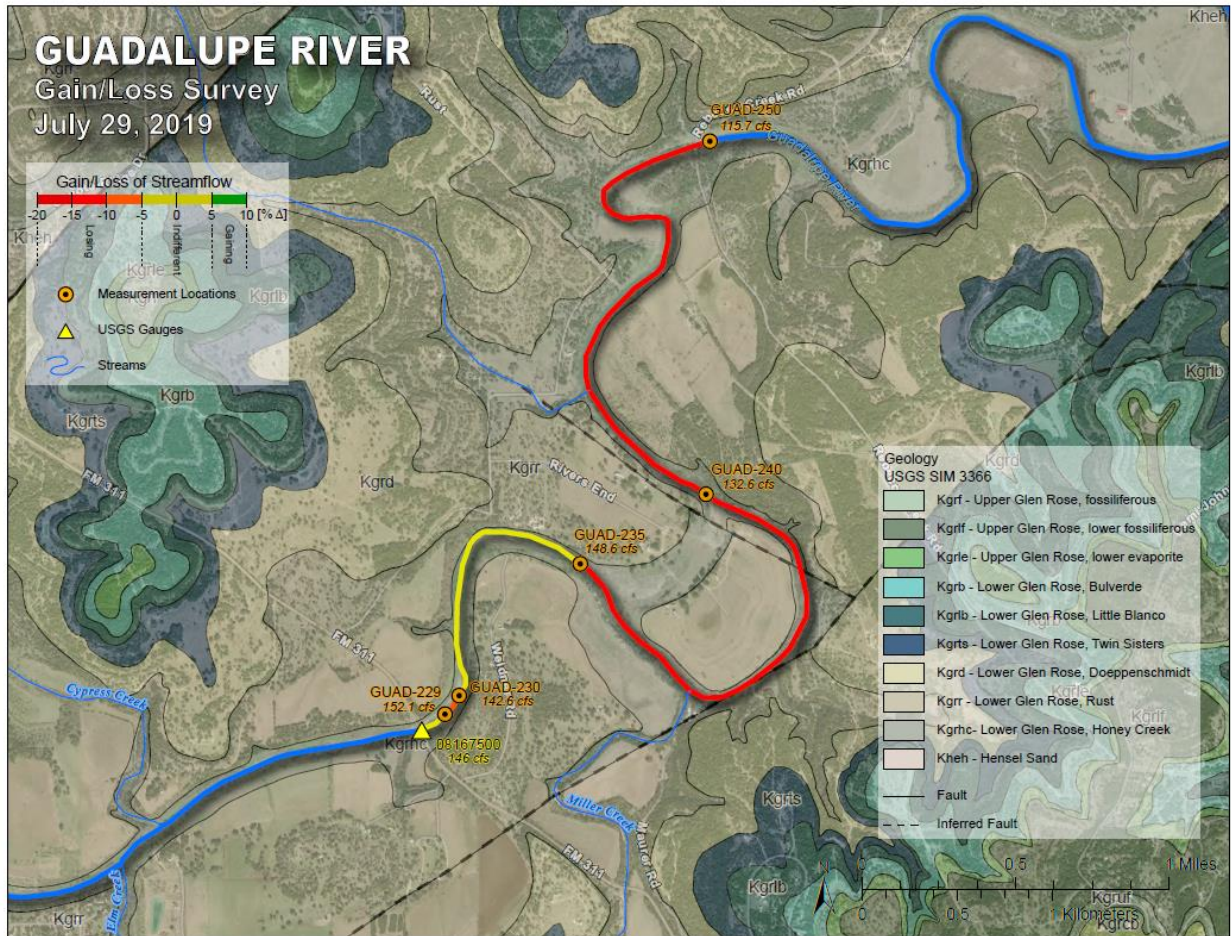


Fig. 3.9 Gain/Loss survey results on the Guadalupe River, July 2019 from USGS gauge to GUAD 250, which shoes 30.3 cfs of loss

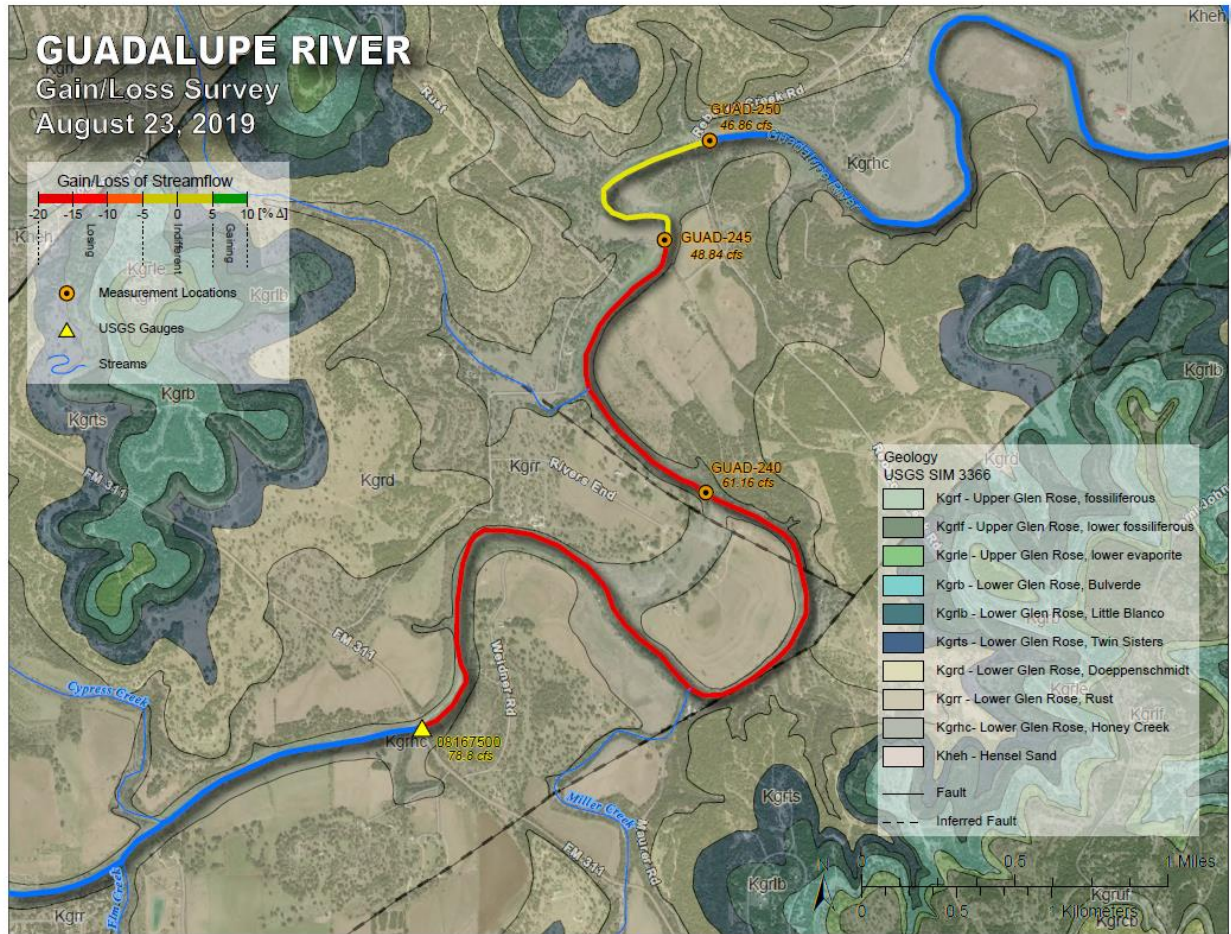


Fig. 3.10 Gain/Loss survey results on the Guadalupe River, August 2019 from USGS gauge to GUAD 250, which shows 31.94 cfs of loss

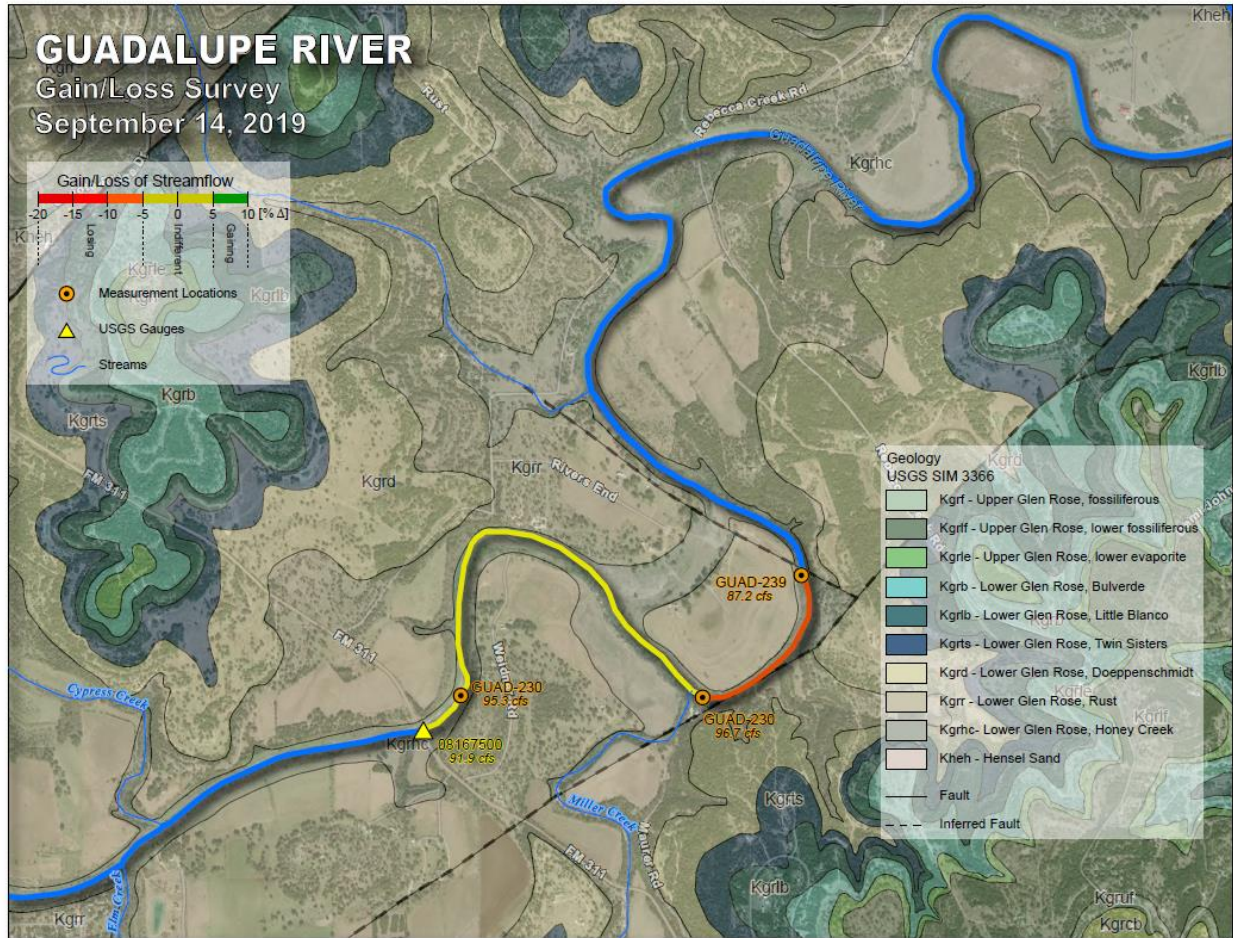


Fig. 3.11 Gain/Loss survey results on the Guadalupe River, September 2019 from USGS gauge to GUAD 239, which shows 9.5 cfs of loss

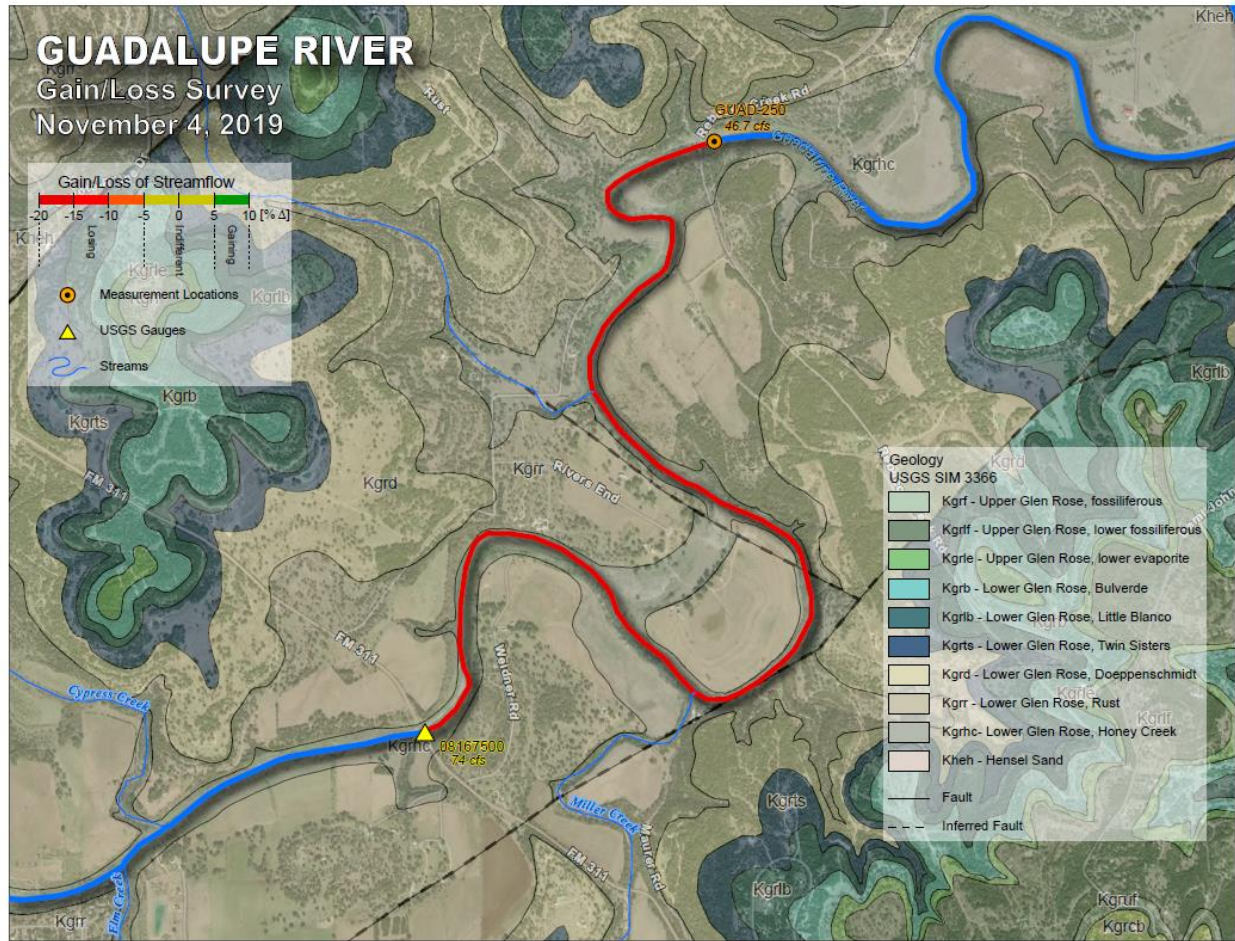


Fig. 3.12 Gain/Loss survey results on the Guadalupe River, November 2019 from USGS gauge to GUAD 250, which shows 27.3 cfs of loss

Upstream Flow at Guad229	Downstream Flow at Guad250	Recharge to Aquifer	Units
146	115.7	30.3	cfs
78.8	46.86	31.94	cfs
74	46.7	27.3	cfs
	Average Recharge	29.8467	cfs

	Total Recharge	335,237,760	cubic feet per year
	Total Recharge	7,696.02	acre-feet per year

Table 3.1 Summary of total discharge, July-November 2019

DISCUSSION

RECHARGE AND DISCHARGE

Table 3.0 summarizes total discharge from July 2019 through November 2019. Results show that the average loss in the Guadalupe River is about 30 cfs, with total recharge in the Guadalupe River basin composing a volume of nearly 7,700 acre-feet. Table 3.1 summarizes all discharge data collected on springs, creeks and the Guadalupe River. It can be noted that discharge is extremely variable, ranging from 2 cfs to 198 cfs. We can interpret these results as meaning that the Guadalupe River basin does, in fact, recharge the aquifer. It should be noted that recharge varies from location to location, as well as between the Guadalupe River, creeks, and springs.

GAIN/LOSS SURVEY

According to the gain/loss maps (Fig. 3.9-3.12), results show that the Guadalupe River was consistently a losing river from July 29, 2019 through November 4, 2019. The percent change in stream flow ranges from +5% to -20%. On July 29, August 23, and November 4, it can be noted that the majority of the river is losing between -10 and -20%. On September 14, the river was still losing up to -10%, but gaining up to +5%. This evidence leads us to interpret the Guadalupe River as a losing stream. In the future, this may have consequences such as the river running dry. In addition, the stream may become disconnected from its groundwater source. A drought could have serious consequences on this river, in that the lack of rainfall could cause the groundwater level to decrease, causing the Guadalupe River to lose even more streamflow than usual.

CONCLUSION

The Karst19 team visited several rivers, creeks, streams, and springs throughout the Guadalupe River Basin. We expected that significant recharge would be present within the Guadalupe River Basin along major faults within the channel and would include major input from karst springs in the watershed. Using ADVs and an ADCP, we found that this is true, as evidence from table 3.0 shows that the Guadalupe River Basin gains approximately 7,700 acre-feet of water each year. Table 3.1 shows that discharge in the Guadalupe River is variable, ranging from 2 cfs to 198 cfs. It is also evident that the Guadalupe River is a losing stream, as proven by figures 3.9-3.12.

CHAPTER IV – Groundwater Levels

The primary objective of this section is to characterize background groundwater levels within the Middle-Trinity Aquifer in the Honey Creek study area for both a snapshot time-frame of late October-early November, 2019 and an annual time-frame. In the effort to achieve this objective, both potentiometric surface maps and hydrographs were created from water-level data sourced from wells in the Middle-Trinity Aquifer. Water level data from the Lower-Trinity Aquifer is also compared and contrasted to data from the Middle-Trinity Aquifer in order to explore how groundwater flow directions and seasonal water level changes differ between the two zones.

BACKGROUND

The Honey Creek study area, located in Western Comal County and Eastern Kendall County, resides within the Hill Country portion of the Trinity Aquifer outcrop. Together with the Edwards Aquifer, the Trinity Aquifer is the primary source of water that supplies for municipal, agricultural, industrial, and recreational uses within the Texas Hill Country region (Sharp and Banner, 1997). The Trinity Aquifer also aids in the sustainability of springs and streams within the region. Because of the Trinity Aquifer's long-term sensitivity to drought and increased well discharge, concerns about groundwater availability for the aquifer have emerged through the years. To help manage groundwater resources, potentiometric surface maps and hydrographs of water level elevations are two available tools that help provide information about groundwater flow paths, potential recharge/discharge areas, and seasonal changes. Several studies have been conducted to help characterize the groundwater to this end in the Hill Country portion of the Trinity Aquifer, including a recently published conceptual model report of the region that contains the Honey Creek study area prepared for the Texas Water Development Board (TWDB) (Toll et al., 2018). Within the Honey Creek study area is the proposed Honey Creek wastewater discharge site, so it is important to establish background water level elevations to help aid in determining how the wastewater discharge site may affect the groundwater/surface water within the study area in the future.

HYDROSTRATIGRAPHY AND GEOLOGIC FRAMEWORK

The Trinity Aquifer is a limestone- and sand-aquifer system characterized in the Texas Hill Country by host-rock permeability, dissolution features, fractures, and fault zones. The Trinity Aquifer within the study area is divided into three zones: (1) the upper zone is within the upper member of the Glen Rose Formation, (2) The middle zone is within the lower member of the Glen Rose Formation and the Hensell Sand/Cow Creek Limestone members of the Pearsall formation, and (3) the lower zone is separated from the middle zone by the confining Hammet Shale member of the Pearsall Formation and is within the Hosston and Sligo Formations (Mace et al., 2000). The Middle-Trinity Aquifer is of primary interest for the purposes of this section as the overall majority of wells within the Honey Creek study area draw from this zone. In a study by Clark et al. (2016), detailed hydrostratigraphic units were defined and mapped within Comal and Bexar Counties (Figure 4.0). Clark has sub-divided the hydrostratigraphic units more than the figure provided by the TWDB. The Honey Creek study area is encompassed by the geographic extent of the study by Clark et al., 2016 and provides a georeference for the surface geology at well sites and approximate thicknesses of units to determine the hydrostratigraphy at the base of each well.

EXPLANATION OF HYDROSTRATIGRAPHIC UNITS		
Group or Formation	Formal and informal member	Hydrologic unit or Informal hydrostratigraphic unit
Taylor Group (Pecan Gap)		Kpg
Austin Group		Ka
Eagle Ford Group		Kef
Buda Limestone		Kb
Del Rio Clay		Kdr
Georgetown Formation		Kg
Person Formation	Cyclic and marine, undivided	Kpcm
	Leached and collapsed	Kplc
	Regional dense member	Kprd
Kainer Formation	Grainstone	Kkg
	Kirschberg evaporite	Kkke
	Dolomitic	Kkd
	Basal nodular	Kkbn
Glen Rose Limestone	Upper Glen Rose Limestone	Kgrc
		Kgreb
		Kgrue
		Kgruf
		Kgrlf
	Lower Glen Rose Limestone	Kgrle
		Kgrb
		Kgrlb
		Kgrts
		Kgrd
Kgrr		
Kgrhc		
Pearsall Formation	Hensell Sand	Kheh
	Cow Creek Limestone	Kcccc
	Hammett Shale	Khah

Figure 4.0. Hydrostratigraphic units defined within Comal and Bexar counties and within the Honey Creek Study area (Clark et al., 2016)

WELL LOCATIONS

As part of the scope of this study, 23 wells within the Honey Creek study area were identified and water level data were either manually collected as part of the karst hydrology course through the efforts of the Edwards Aquifer Authority (EAA), or were obtained through network databases through the efforts of the Comal Trinity Groundwater Conservation District (GCD) and their WellIntel monitoring network, and the waterdatafortexas.org continuous water level data. The wells within the study area are located within the western portion of Comal County and the eastern portion of Kendall County (Figure 4.1) (Table 4.0). Sites include residential, state monitoring wells, and others. These wells were selected on the basis of their proximity to Honey Creek and the relationship with the proposed Honey Creek wastewater discharge facility.

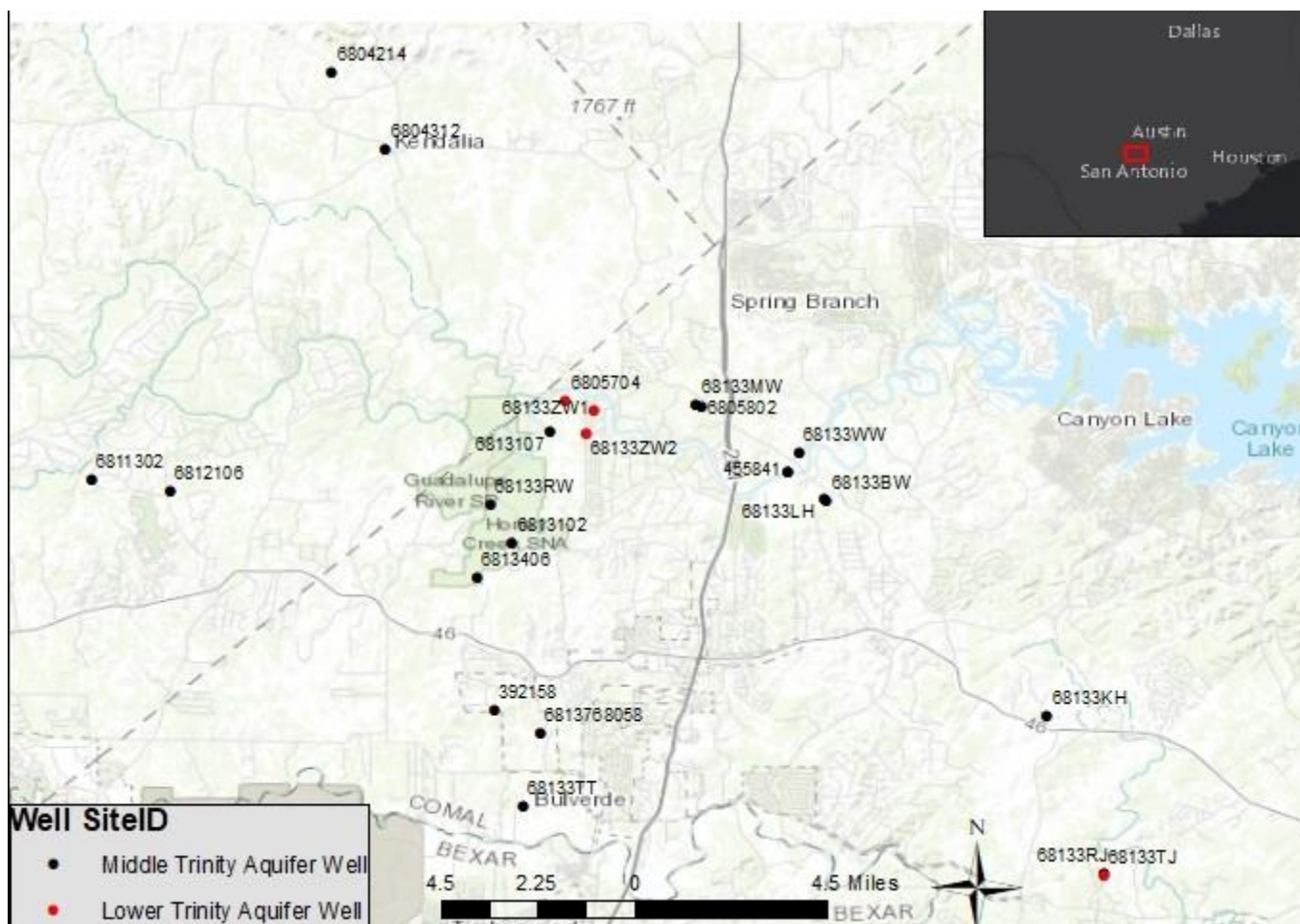


Figure 4.1. Locations of the 23 wells in which water level data were obtained, labeled by SiteID/state well number, within the Honey Creek study area.

NAME	Well_ID	Lat.	Long.	Date	Surface Elevation (ft.)	Water Level Elevation (ft.)	Well Depth (ft.)
Larry Hull's House Well (CTGC04)	68133LH	29.85223	-98.376804	11/2/2019	1067.039	903.329	260
Bunny Warren's House Well (CTGC01)	68133BW	29.85133	-98.375751	11/2/2019	1072.004	903.042	260
Windmill Well	68133WW	29.86746	-98.385268	11/2/2019	1001.803	No data	No data
Barbed Wire Well	455841	29.86132	-98.388832	11/2/2019	1009.41	944.24	243
Hand Pump Well	68133HW	29.86131	-98.389199	11/2/2019	1009.283	945.673	No data
H.L. Saur's well (CTGC02)	6805802	29.88308	-98.418142	10/28/2019	1122.342	1026.412	220
Dr. K. Higby well (CTGC03)	68133KH	29.7785	-98.301423	11/2/2019	1284.543	784.02	No data
Feresia & Rob Johnson well (CTGC05)	68133RJ	29.72553	-98.2821	11/2/2019	1089.403	745.05	540
Feresia & Rob Johnson well (CTGC06)	68133TJ	29.72487	-98.2819	11/2/2019	1079.036	621.99	1100
Tom Turk well (CTGC07)	68133TT	29.74773	-98.478973	11/2/2019	1131.091	872.34	No data
TPWD - Rust Windmill	68133RW	29.85022	-98.490083	11/6/2019	1175.286	1101.736	No data
Lea Anzalotta well	6813768058	29.77287	-98.47319	11/5/2019	1255	951.2	445
Scott Pegues well	392158	29.78048	-98.48831	11/5/2019	1370	992.9	600
Cow Creek GCD well 1	6812106	29.85461	-98.598611	11/5/2019	1234	1134.88	255
Cow Creek GCD well 2	6811302	29.85864	-98.625083	11/5/2019	1308	1142.98	295
Cow Creek GCD well 3	6804312	29.97042	-98.525333	11/5/2019	1367	1248.68	310
Cow Creek GCD well 4	6804214	29.99611	-98.543889	11/5/2019	1479	1316.98	400
Zerep well - Windfrey Dr.	681332W1	29.88222	-98.454771	10/28/2019	1081.529	1042.479	481
Zerep well - Winding River	681332W2	29.87384	-98.457323	10/28/2019	1133.27	847.37	500
Murphy Well	68133MW	29.88363	-98.420227	10/28/2019	1170	1020.32	300?
GRR 2 - Main ranch well (LT)	6813107	29.87491	-98.469672	10/25/2019	1185	928.6	336
TPWD - Residence	6813406	29.82518	-98.494547	10/25/2019	1253	1079.47	225
State Natural Area Water Well	6813102	29.83702	-98.482489	11/6/2019	1216.931	1079.831	200
Guadalupe River Ranch) Old House V	6805704	29.88514	-98.464262	9/25/2019	1099	923.69	315

Table 4.0. Well Site Information in the Honey Creek Study Area.

Since the scope of this study is minimal with respect to the number of water level data obtained and assessed, it is important to give an indication of the actual number of wells within the study area in order to provide a reference for the potential of well discharge in the area and to demonstrate the limitations of analyzing fewer wells through the creation of potentiometric surface maps. It is worth noting that a subdivision north east of the Honey Creek State Natural Area (SNA) has recently expanded and includes individual wells for each property located within a geographically dense area.

METHODS AND DATA

MANUAL WELL MEASUREMENTS

As part of this study, 6 different individual wells, proximal to the intersection between the Guadalupe River and FM 311, were accessed for manual water level measurements by the karst hydrology course within the Honey Creek study area through the efforts of the Edwards Aquifer Authority and the Comal Trinity Groundwater Conservation District. The first task at each well involved collecting geographic coordinates and surface elevation data adjacent to the well. A Leica Zeno 20 Multi-GNSS Triple-Frequency Compact Antenna attached to a Seco telescoping bipod was used for this purpose (Figure 4.2). The GPS coordinates were referenced to the World Geodetic System 1984 (WGS84) datum, and elevations were recorded in feet above mean sea level (MSL). Elevation data accuracy ranged between 0.08-0.13 ft. across the different well sites. It was noted that depending on the presence of vertical obstructions such as trees and utility lines, GPS accuracy had the potential to diminish.



Figure 4.2. The Leica RTK receiver and bipod adjacent to a residential well site in the Honey Creek study area as a water level measurement is being taken

After establishing a land surface elevation datum for each well site, the class next measured and recorded the measuring point (MP), the distance between the land surface to the top of the well access point. To measure the depth to water, the class primarily used an “E-line”, Heron Instruments Inc. Skinny Dipper Water Level Meter (Figure 4.3). Secondly, an RGI Model 300 Sonic Water Level Meter was used at one of the wells to compare to the water level measurement taken with the E-line (Figure 4.3). To this end, 7 measurements were conducted with the sonic meter, and the average depth to water level with the sonic meter was about 0.67 ft. greater than the value recorded with the “E-line”. Comparing the two methods, it was noted that measurements taken with an “E-line” tend to have a higher degree of accuracy, so the “E-line” was the tool used to collect manual water level measurements for the additional wells for this study.



Figure 4.3. E-line and sonic meter being used to take depth to water level measurements at a residential well in the Honey Creek study area

The depth to water (DTW) data were recorded for each well that was visited, and a water level elevation was computed by adding the MP data to the land surface elevation data and subtracting from that sum the DTW data. 8 additional manual water level elevation measurements were obtained for wells in the Honey Creek study area through the efforts of the EAA and Dr. Marcus Gary. All together, manual water level measurements were taken between

a time period of 10/25/19-11/06/2019. These data were transcribed into a database that contains fields for GPS coordinates, land surface elevation, DTW, water level elevation, and other additional fields containing metadata about each well site. 2 of the 13 wells in which manual water level measurements were equipped with WellIntel remote sensing water level technology and continuous water level data were also obtained for these wells.

ADDITIONAL WATER LEVEL MEASUREMENTS

Of the remaining 9 wells in which data were obtained and utilized for this study, 4 came from well sites within the Cow Creek GCD where continuous water level data were obtained from the waterdatafortexas.org interactive database. The remaining 5 well site continuous data were sourced through the WellIntel database with cooperation from the Comal Trinity GCD.

HYDROSTRATIGRAPHIC UNIT DETERMINATION

To distinguish which zone of the Trinity Aquifer each well was located in, the well locations were first plotted within ArcMap v.10.6.1 on the Clark et al., 2016 surface hydrostratigraphic unit shape file. Well depths were obtained for 19/22 of the well sites through the Submitted driller report database, TWDB groundwater database, and other sources. From the well depth data, the hydrostratigraphic unit at the base of the well was estimated based on the average thickness of each hydrostratigraphic unit provided by the study by Clark et al., 2016. Since the margin of error was large based on extrapolation of uncertainty of the exact unit thicknesses, the exact hydrostratigraphic unit for each well within the study is tentative. However, the zones of the Trinity Aquifer for each well were clearer. Altogether, it was estimated that 19 of the wells occurred in the Middle-Trinity Aquifer, and 4 of the wells occurred in the Lower-Trinity Aquifer. Information about the screened interval for the majority of the wells were not located as part of this study, so the hydrostratigraphic unit depth determination was based off of total well depth instead.

POTENTIOMETRIC SURFACE MAP

To determine a general trend of groundwater elevation within the Honey Creek study area, point elevation data for 19 wells (both manually collected data and remote sensing data) in the Middle-Trinity Aquifer and 4 wells in the Lower-Trinity Aquifer were imported into ArcMap v.10.6.1. Using the Kriging algorithm interpolation tools within ArcMap v.10.6.1, a potentiometric surface raster file was created from the individual point data. The Kriging interpolation method is well suited for cases in groundwater hydrogeology where the data are spatially correlated with distance (Jie et al., 2013). Contours were then applied to the potentiometric surface raster in the study area through the use of the contouring tools in ArcMap v.10.6.1. At this point, contours have not been manually adjusted to account for the presence of faults, hydrogeologic boundaries, preferential flow paths, etc.

HYDROGRAPHS

To model the changes in water elevation within the study area, individual hydrographs were created for each well that provided continuous water level data. A total of 11 wells within the Honey Creek study area had corresponding continuous water level data. Of these 11 wells, 7 data sets came from the WellIntel database with cooperation from the Comal Trinity GCD. The

remaining 4 data sets came from well sites within the Cow Creek GCD. All graphs were created using Microsoft Excel, plotting time vs. water elevation spanning over the past year. In some cases, continuous data was not available from the beginning of the year; these graphs show the data that had been provided.

DRAWDOWN CURVE

A drawdown curve for State Well Number 68-13-102 was created using static water level data. While pumping was occurring at the well, manual water level measurements were recorded over a time period of approximately two hours on 9/28/2019. These data were transcribed into a database that contains fields for land surface elevation, measuring point, DTW, water level elevation, and well depth for this specific well site. The drawdown curve was created using Microsoft Excel, plotting time vs. water elevation.

RESULTS

POTENTIOMETRIC SURFACE MAPS

For the static water level data from 19 wells within the Middle-Trinity Aquifer, water elevations ranged from 745.05 ft to 1316.98 ft. above MSL. This change occurred over a geographic distance of about 30 miles within the study area. A general trend of decreasing water level elevation within the Middle-Trinity Aquifer is seen from northwest to southeast within the study area (Figure 4.4). In addition to this overall trend there is a smaller trend of decreasing water level elevations into the Honey Creek State Natural Area/ Guadalupe River State Park from both the northwest and southeast.

For the static water level data from all 4 wells within the Lower-Trinity Aquifer, water level elevations ranged from about 621 ft. to 1043 ft. above MSL for the study time-period of 10/25/19-11/06/2019 (Figure 4.5). The three wells northeast of the Honey Creek SNA and Guadalupe River State Park have water level elevations that range from about 847 ft. to 1043 ft. above MSL. The 1 well in the far southeast of the study area has a significantly lower water level elevation of about 622 ft.. This well was the deepest of all wells that were used for this study with a depth of about 1100 ft. above MSL.

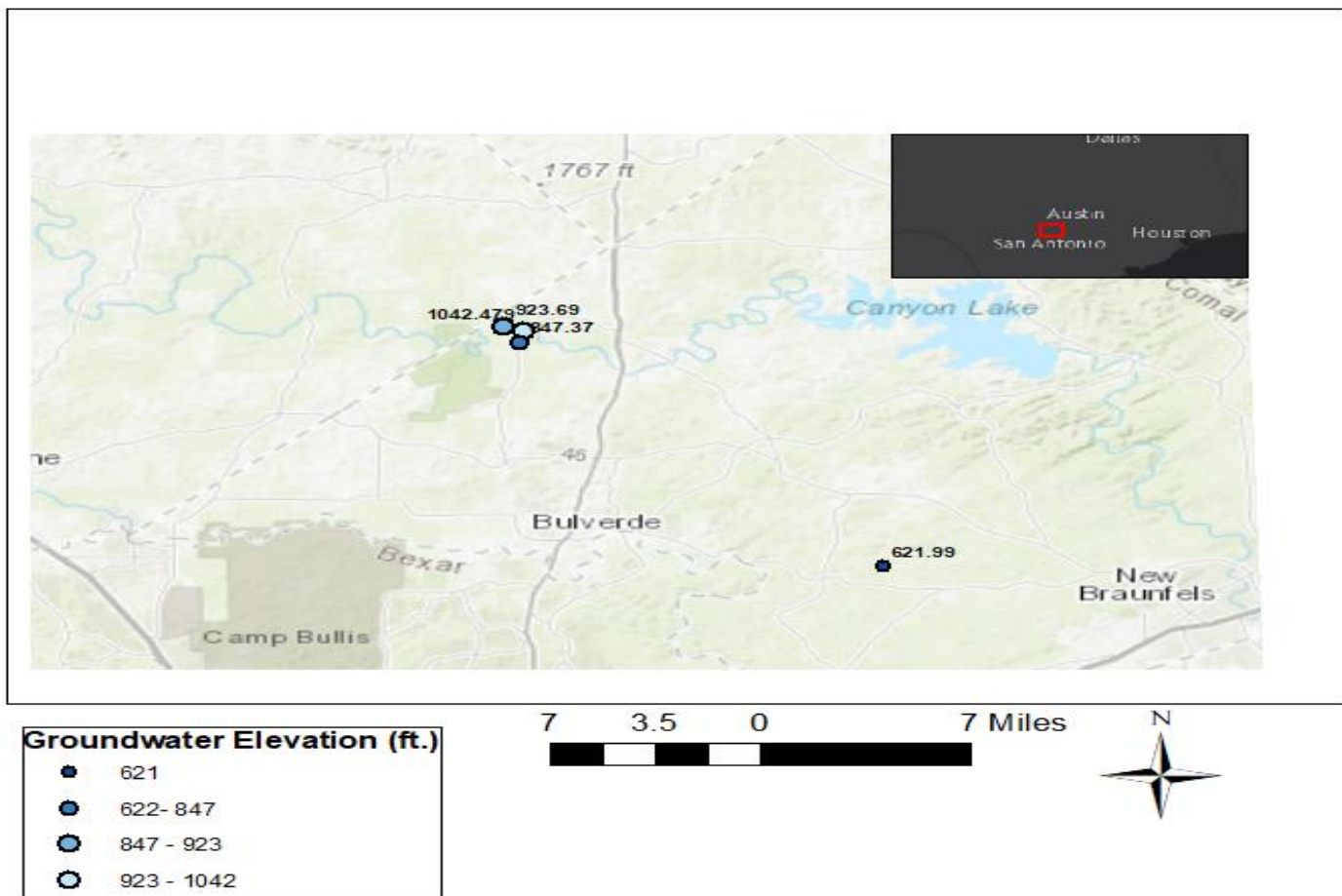


Figure 4.5. Lower-Trinity Aquifer water level elevations

HYDROGRAPHS

As seen in the hydrographs for the continuous water data within the Middle-Trinity Aquifer, there is a general correlation in water elevations throughout the past year from wells within the same hydrogeologic strata (Figure 4.6). Water level elevations in this particular region ranged from 745.05 ft. to 1316.98 ft. above MSL (Appendix 4.1). These results affirm the conclusions drawn from the potentiometric surface maps: there is a regional trend of decreasing water level elevations from the northwest to the southeast.

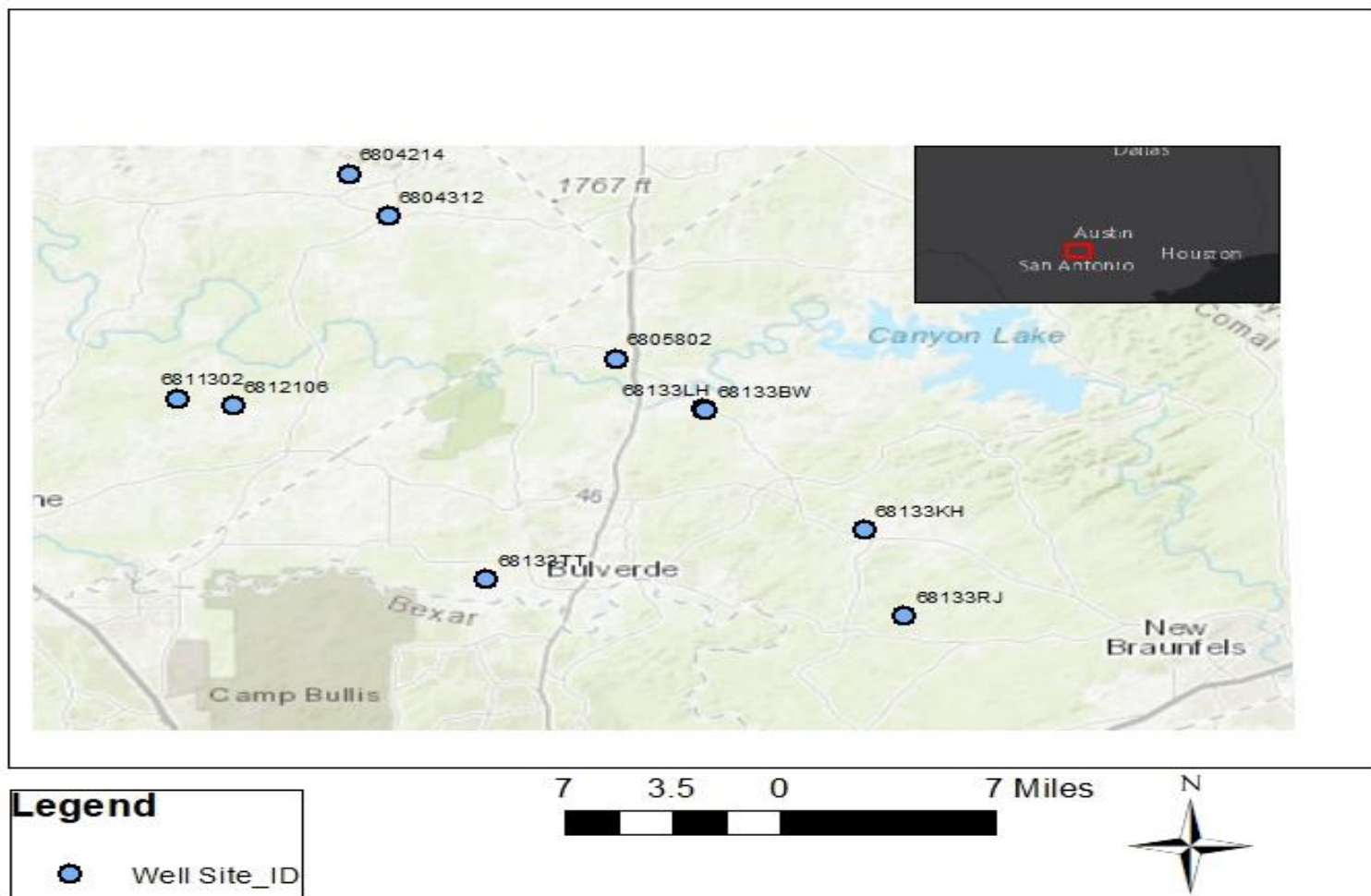


Figure 4.6. Map of Well Sites within the Middle-Trinity Aquifer of the Honey Creek study area, Comal County, Texas. Hydrographs were created from continuous water elevation data for this site (Appendix 4.1).

One continuous monitoring well, 68133TJ, within the Honey Creek study area was determined to be within the Lower-zone of the Trinity Aquifer. Of the wells with continuous water level data, this well was the deepest at 1100 ft. Water level elevations at this well fluctuated from approximately 580 ft. to approximately 680 ft. above MSL (Figure 4.7) (Appendix 4.2). This site began continuous water level data collection in March of 2019; since then, there has been an observable declining trend in water elevation from northwest to southeast, as depicted in the hydrograph.

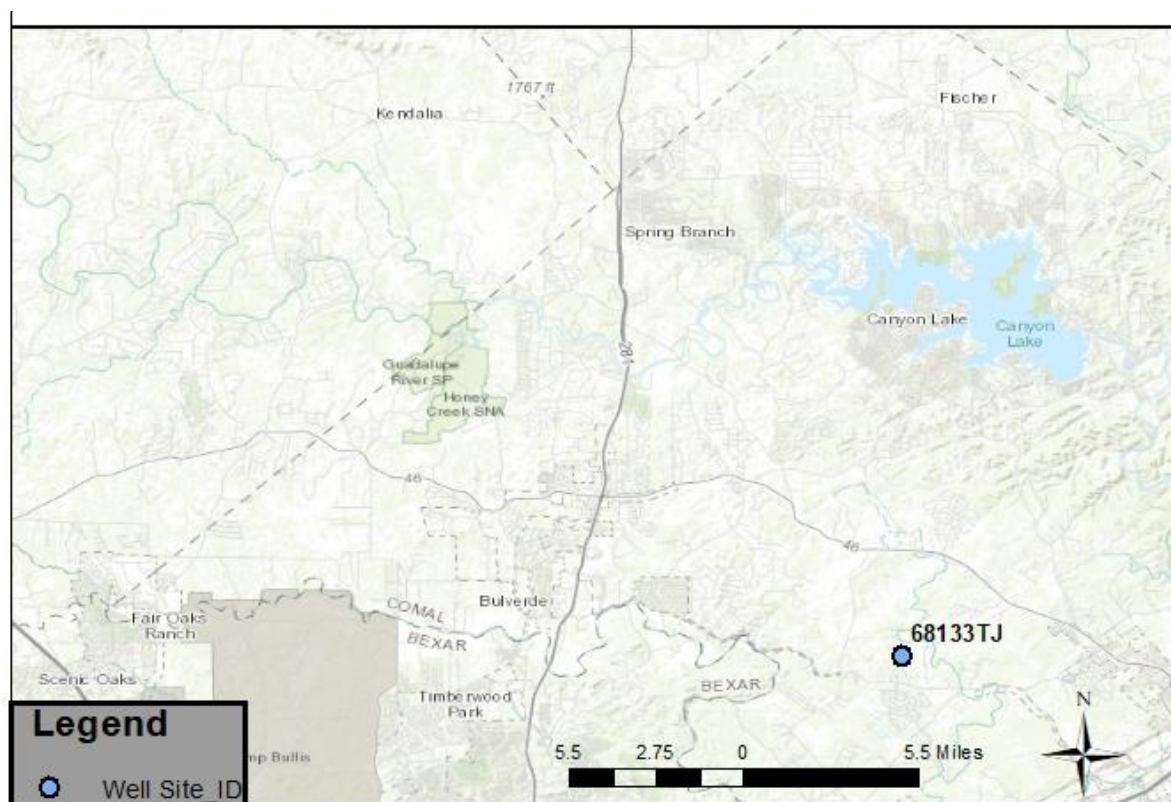


Figure 4.7. Map of Well Sites within the Lower-Trinity Aquifer of the Honey Creek study area, Comal County, Texas. Hydrograph was created from continuous water elevation data for this site (Appendix 4.2).

When comparing the hydrographs of the Middle- and Lower-Trinity Aquifers, a common trend of declining water elevation is observed across the study area, with decline from the northwest to southeast.

DRAWDOWN CURVE

The drawdown curve for well 68-13-102 shows the effect that continuous pumping has on that particular well within the Middle-Trinity Aquifer (Figure 4.8). Manual water level elevations measurements were taken over a time period of two hours on 9/28/19. The water elevation was at its peak at 8:53 AM, with a pre-pumping water elevation of 1081.77 ft. Several rounds of pumping ensued; once pumping stopped and the well reached a static state, water level

elevation had dropped to 1031.93 ft. These values account for a 49.84 ft drop in water elevation over a time period of one hour and nine minutes. When the last measurement was taken at 10:40 AM, the water level had begun to recover.

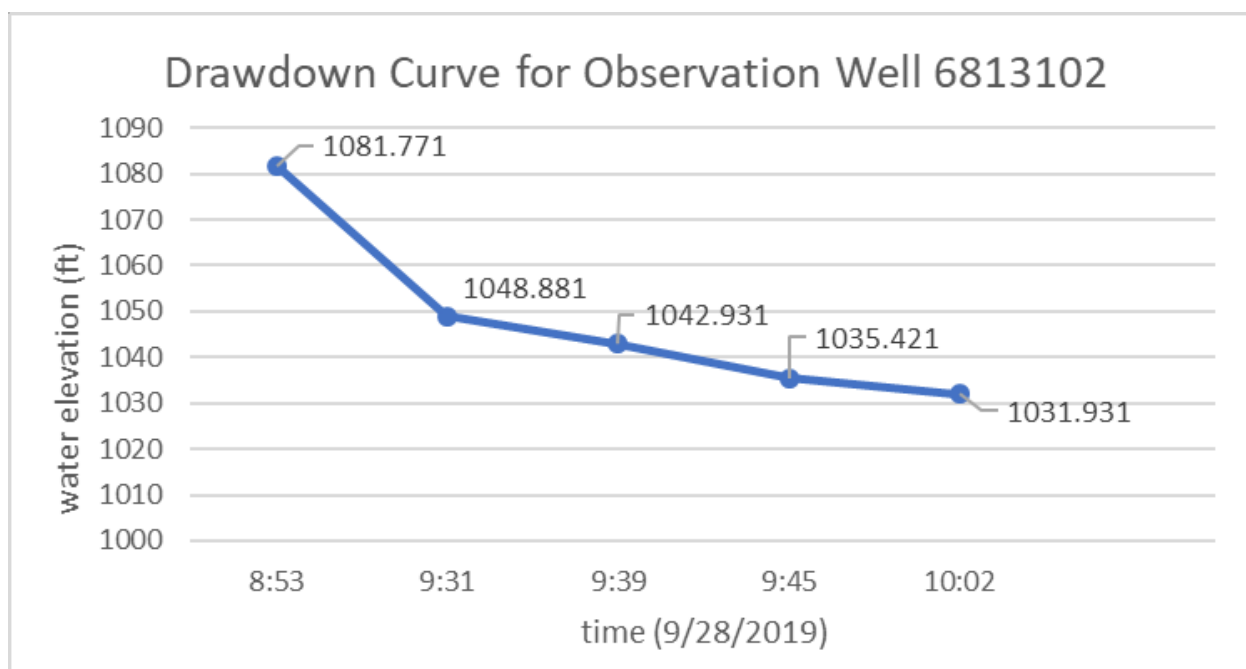


Figure 4.8. Drawdown Curve of Well 68-13-102 in the Middle-Trinity Aquifer within the Honey Creek study area, Comal County, Texas. Curve was created from multiple manual water elevation measurements.

DISCUSSION

POTENTIOMETRIC SURFACE MAP

The potentiometric surface map for the Middle-Trinity was created from water level elevation data from 19 well sites (Figure 4.4). The time period that these water level elevation data were sourced from was 10/25/19-11/06/2019. The general overall trend of decreasing water level elevations from the northwest to the southeast within the study area may cause a regional groundwater flow path within the study area. For the case of the Middle-Trinity Aquifer, there appears to be a possible depression in water level elevations around the Honey Creek SNA and Guadalupe River State Park. This may be explained as a potential area of preferential recharge for the study area because as we discovered, the area is defined by karst caves/conduits. While there was limited data for water level elevations for the Lower-Trinity Aquifer as part of this study, there was a smaller trend of water level elevation decline from southwest to northeast in the 3 wells near the Guadalupe River. However, a potentiometric surface map was not created from the limited data. Comparing the potentiometric maps for the Middle-Trinity Aquifer to a previous 2018 TWDB conceptual model report, the same northwest to southeast decreasing water level elevation trend is evident by the water elevation contours (Figure 4.9).

Conceptual Model Report for the Hill Country Trinity Aquifer
 Groundwater Availability Model

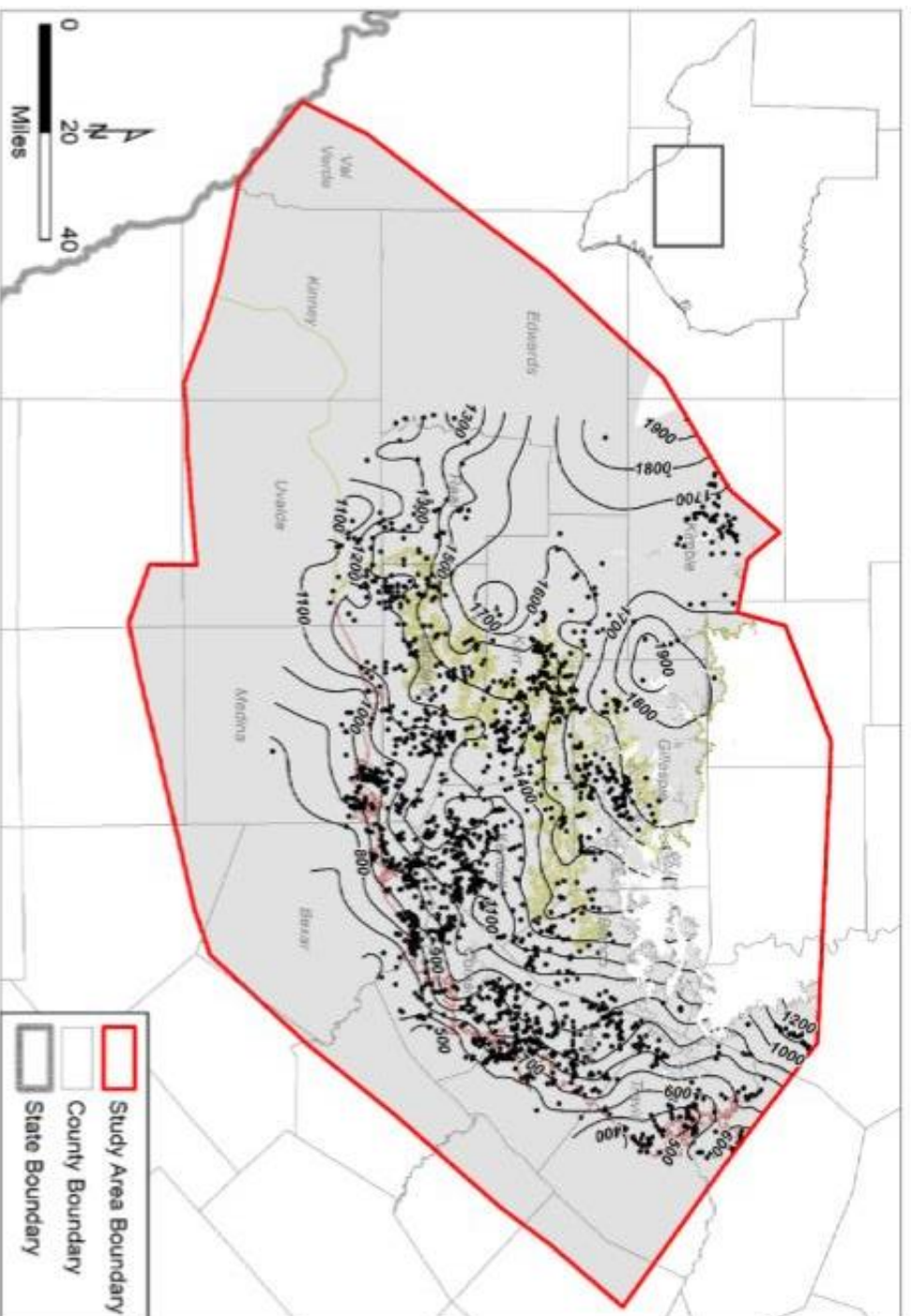


Figure 4.9. Potentiometric surface map for the Hill Country Trinity portion of the Middle-Trinity Aquifer. The Honey Creek study area portion of the map shows a similar water level elevation change trend as the map created for this study (Troll et al., 2018)

It is important to note that these maps were generated from limited data compared to studies that have a much higher resolution of data with more water level elevation control points. For the purposes of understanding a relatively small study area such as the Honey Creek study area, this amount of water level elevation data may be sufficient, but it is likely rarely consequential to obtain more data for a study area if possible. There is also propagated error from the estimation of the hydrostratigraphic units that each of the 23 wells occupy. For several cases, the bottom of the wells were located near the Hammett Shale boundary that separates the Middle- and Lower-Trinity Aquifer. It is therefore relatively uncertain which wells are exactly within which hydrostratigraphic units. This process may be refined with more information about the completion of the wells. Limitations of this study also include the use of the Kriging interpolation algorithm on its own in ArcMap v.10.6.1. With more well control points the interpolation could be improved however more important considerations likely include manual readjustment of the contours based on information about the hydrogeologic boundaries (Honey Creek, Guadalupe River), faults, and preferential flow paths within the study area. Therefore, with these considerations, the potentiometric surface maps should not be taken at face-value to represent the complete reality of groundwater flow paths. However, the water level elevation data collected as part of this study are valuable for future studies and expansions of this study.

HYDROGRAPH

The hydrographs for the Middle- and Lower-Trinity Aquifer were created from continuous water level data provided from the Cow Creek GCD and the WellIntel database with cooperation from the Comal Trinity GCD (Figure 4.6 & 4.7) (Appendix 4). Similar to the potentiometric maps, the general decline in water level elevation within this region illustrated by the hydrographs could be explained by regional groundwater flow paths, with decline from the northwest to the southeast.

Of the well data provided by the Cow Creek GCD, wells 6812106 and 6811302 are closely correlated. The wells reach a depth of 255 ft. and 295 ft., respectively. When observing the hydrographs of these wells, both have steep rising limbs culminating in peaks of 1152-1155 ft. around times 1/9/2019 and 5/9/2019. These could be attributed to seasonal events; seasonal changes, including changes in precipitation, could account for the slight rise in water elevation during these traditionally rainy months. The graph of well 6812106 has shallower falling limbs than well 6811302. The difference in recovery times could be attributed to the hydrogeological properties of the area; varying properties within the subsurface can influence recharge rates and preferential flow paths. Well 6812106 has a longer lag time and greater variation in water levels, generally spanning a range of 1135-1145 ft. Well 6811302 is fairly consistent, stabilizing relatively quickly around a range of 1140-1145 ft. after precipitation events occur. This suggests that the subsurface varies slightly in geologic and hydrologic properties, despite the two well sites being relatively close to each other.

Of the wells provided by the Comal Trinity GCD, wells 68133LH and 68133BW are very closely correlated. These two wells are in close proximity to each other and lie within the same stratigraphic unit of the Middle-Trinity aquifer at a depth of 260 ft. When observing the hydrographs, both sites respond to changes in the same fashion and at the same rate. Because of their close proximity, changes in one well, such as the onset of pumping, can be seen in the other, even if not directly affected.

Also provided by the Comal Trinity GCD are wells 68133RJ and 68133TJ. These wells, while in close proximity to each other, reach varying depths of 540 and 1100 ft., respectively. The variation in depth puts these two wells in different zones of the Trinity aquifer; well 68133RJ is located in the Middle-Trinity while well 68133TJ is in the Lower-Trinity. When considering the Lower-zone of the Trinity Aquifer, there was a limited amount of data to draw definite conclusions; the lack of data for this zone makes it difficult to determine any definitive regional trends based on seasonal or temporal changes. Despite this, both wells 68133RJ and 68133TJ are still significant since they show how varying depth and stratigraphic units have an impact on groundwater elevation. When looking at the hydrograph of the single well that data was provided for in the Lower-Trinity, 68133TJ, the general trend was consistent with the regional declining trend of the Middle-Trinity.

Another trend that was observed was rapid drawdown and recovery over a fixed interval. Such rapid fluctuations in water elevation in a single well could be explained as pumping events for residential use, as seen in well 6804312. Overall, the graphs generated from this data are limited, as some wells had only begun continuously monitoring as recent as October 2019; these data sets were inconsistent with the surrounding wells, which had data spanning as far back as a year prior.

DRAWDOWN CURVE

The drawdown curve for well 68-13-102 can be used to show the effects that pumping water from a well has and how it might affect the behavior of the Middle-Trinity Aquifer (Figure 4.8). The data used to create the drawdown curve was limited, as only 6 manual water level measurements were used to generate the graph. More data points would be beneficial, as the drawdown would be more accurately tracked through time. Specifically, additional data during recovery of the water level elevation would reflect a more accurate curve. To get a better understanding of the Middle-Trinity Aquifer, recovery tests could be conducted at the various well sites within the study area to estimate aquifer properties such as hydraulic conductivity.

CONCLUSIONS

The potentiometric maps, hydrographs, and drawdown curve all help to provide a general characterization of the groundwater conditions in the Honey Creek study area. Some conclusions from this study include:

- There is an overall regional trend of groundwater flow from northwest to southeast within both the Middle-Trinity Aquifer
- Preferential recharge zones for the Honey Creek study area may exist in the Honey Creek State Natural Area/Guadalupe River State Park area.
- There is a general decline in water level elevation within both the Middle- and Lower-Trinity Aquifer, with observable seasonal changes as precipitation occurs.
- The drawdown curve/recovery test method could be applied to various wells within the Honey Creek study area to get a more accurate depiction of Middle-Trinity Aquifer properties.

CHAPTER 5 – Water Quality

The objective of this section is to characterize the background water quality of the Honey Creek area. Water samples from multiple public and private use wells, two natural springs, and two sites on the Guadalupe River were taken to achieve this objective. Chemical constituents of interest include major and minor ions, nutrients, and isotopes (carbon, oxygen, and hydrogen). Chemical contaminants of interest include PFAS, personal care products, and pharmaceuticals (PPCPs).

BACKGROUND INFORMATION

The study area is mostly composed of karst limestone. This type of geology means that significant concentrations of bicarbonate, magnesium, and calcium are expected (Mahler et al., 2008). A study done by Fahlquist et al. (2004) determined that the hydrochemical facies for the Trinity aquifer ranged from calcium-magnesium-bicarbonate-chloride-sulfate to sodium-chloride-sulfate-bicarbonate.

Due to the pending wastewater permit at this study site, nutrient concentration is of significant interest. Nutrients are defined as chemical constituents that are essential to the growth of organic organisms (Mabe 2007). Excessive algae growth from elevated levels of the nutrients nitrogen and phosphorus can cause eutrophication (Mahler et al., 2008). Eutrophication is when the concentration of dissolved oxygen declines as it is consumed by algae decomposition. This is detrimental for other aquatic life that depend on dissolved oxygen. In addition to this, excess growth of algae can also cause problems for recreational and industrial use of surface water by clogging pipes and waterways (Mahler et al., 2011).

Percent modern carbon (pMC), carbon-14, and the delta ratios of D/H, O18/O16 were the isotopes used in this report. Isotopes in water can indicate flow paths, phase change, and chemical reaction extent (Sidle, 1997). Carbon-14 in dissolved inorganic carbon (DIC) is often utilized in determining the age and residence time of groundwater (Gillon et al., 2009). Carbon-14 and pMC were used together to analyze the relative ages of the water samples.

Elevated concentrations of PFAS, personal care products and pharmaceuticals (PCPPs) are possible in central Texas, especially in areas experiencing rapid population growth. Per- and polyfluoroalkyl substances (PFAS) are a group of chemicals that are mainly used as water and stain repellents. It has been proposed that the buildup of these compounds in humans can have many adverse health effects (U.S. Environmental Protection Agency, 2018). As a result, PFAs have been of particular concern in recent years.

METHODS

SAMPLE COLLECTION

For this study, water samples were collected in six wells, two springs and two sites in the river (Table 5.0). This section describes the methodology followed for water quality sampling in these sites.

Site ID	NAME	Site Type
68-13-102	State Natural Area Water Well	Well
68-05-705	SW GUAD 200	River
68-12-302	Public Water Supply GSP	Well
68-13-103	Honey Creek Cave Spring	Spring
68-13-105	Little Honey Creek Spring	Spring
68-05-704	GRR Main House Well 3	Well
68-05-807	Meyer Well #2	Well
68-13-107	GRR Main House Well 2	Well
68-13-210	SW GUAD 212	River
68-13-406	TWBD Residence Well (MT)	Well

Table 5.0. Stations where water quality samples were collected.



Figure 5.0. Students inserting e-line into well to measure depth to water.

First, a pump was used in order to collect water samples the well. The well was purged three times its total volume to ensure it was reflective of the aquifer. Next, a pump was used to collect water samples the well. The well was purged three times its total volume to ensure that the samples were representative of the aquifer. The tube in the pump was then decontaminated with liquinox and then with DI water to minimize the risk of accidental contamination, since the tube had been used in previous wells that the water was reflective of the aquifer. The tube in the pump was then decontaminated with liquinox and then with DI water to minimize the risk of accidental contamination.



Figure 5.1. Well pump and generator seen on the back of a truck.



Figure 5.2. Pump inserted into well after the decontamination process

Prior to the water quality testing, the chain of custody form was completed (seen in the Appendix 5). The Eureka manta 30 was used to measure temperature, conductivity, Ph, dissolved oxygen and turbidity. Figure 5.3 shows the probe used in the sampling.



Figure 5.3. Eureka Manta 30 probe.

The probe was first calibrated for conductivity, pH and turbidity. First, the probe was rinsed three times with Deionized Water. Since the values used to calibrate are project dependent, we used the limit values that are commonly reported in the Edwards aquifer to be sure that our measurements were accurate. The values are shown below.

- Conductivity (mV): 600 and 1200
- pH: 4, 7 and 10
- Turbidity: We used Deionized Water to calculate turbidity

The bottles for water quality sampling were previously prepared and labeled (with (1) type of sample, (2) preservatives when applied and (3) volume) in the laboratory. Before sampling we

labeled the bottles with the (1) Sample ID, (2) Client: Edwards Aquifer Authority, Corpus Christi or Houston and date. Figure 5.4 shows an example of a completed water sample container.

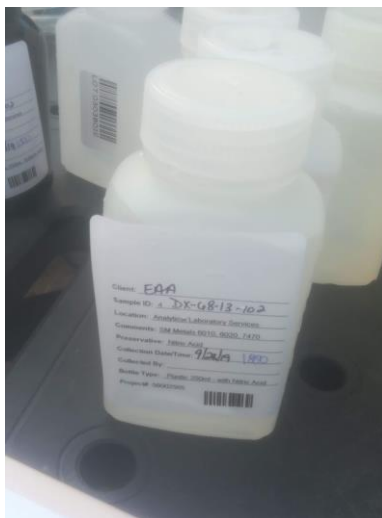


Figure 5.4. Example of water sample sent to chemical analysis laboratory.

Our chemical analysis included testing for:

- Total Organic Carbon
- Stable Isotopes (bottles were rinsed before collecting)
- Dissolved Inorganic Carbon (bottles were rinsed before collecting and samples were filtered)
- ^{13}C and ^{14}C (bottles were rinsed before collecting and samples were filtered)
- Alkalinity (these samples were filtered)
- Metals (these samples were filtered)
- Dissolved Organic Carbon (these samples were filtered)
- Pharmaceuticals

Once collected, the samples were iced in coolers at temperatures requested by the analytical laboratories.



Figure 5.5. Organizing the sample containers.

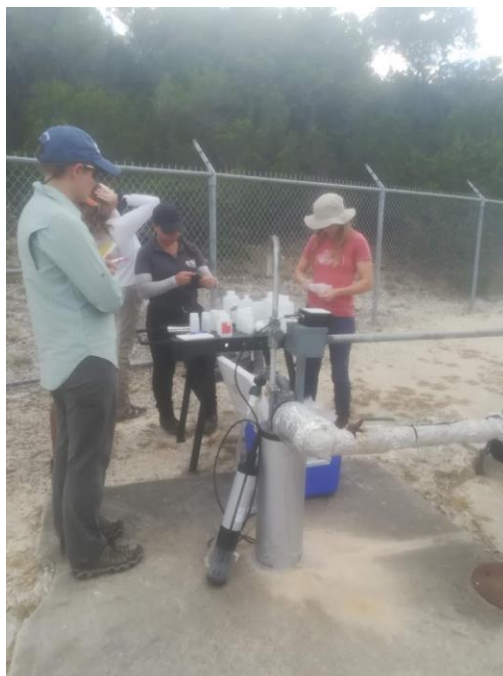


Figure 5.6. Samples being taken and organized from well.

For testing streams and springs, the same equipment (probe manta 30) was used for measuring temperature, pH, conductivity, dissolved oxygen and turbidity. This time we used the stream sampling case, which allows to collect the data directly in the stream/spring. Unlike the well samples, the water quality samples were collected by submerging the bottles (previously prepared and labeled) into the water or by using a bailer for the samples that required to be filtered.

ANALYTICAL METHODS

MAJOR IONS

For testing streams and springs, the same equipment (probe manta 30) was used for measuring temperature, pH, conductivity, dissolved oxygen and turbidity. This time we used the stream sampling case, which allows to collect the data directly in the stream/spring. Unlike the well samples, the water quality samples were collected by submerging the bottles (previously prepared and labeled) into the water or by using a bailer for the samples that required to be filtered

A Piper diagram (figure 5.9) was used to study the similarities and differences in the composition of the waters sampled in the study area and to classify them into certain chemical types. In the Piper diagram, major ions are plotted in the two base triangles as cation and anion milliequivalent percentages. The diamond field represents the total ion relationship (Chadha, 1999). The cations and anions concentrations used to build the Piper Plot are presented in Table 5.1 and included in the project database.

Site ID	Cations				Anions		
	Ca (ug/L)	Mg (ug/L)	Na (ug/L)	K (ug/L)	Cl (mg/L)	SO4 (mg/L)	CaCO3 (mg/L)
68-13-102	84900	15200	5900	8340	14.3	26.7	266.4
68-05-705	57000	21300	12300	1910	24.5	20.4	202.15
68-12-302	41400	35800	214000	12100	298	202	266.9
68-13-103	118000	8190	7000	1140	13.6	7.34	308.4
68-13-105	109000	12400	8510	1190	18.1	11.8	296.9
68-05-704	86900	36500	59100	6730	65.3	58.8	345.75
68-05-807	60600	46200	246000	14300	343	233	262.25
68-13-107	53500	45000	276000	14700	360	251	238.05
68-13-210	54700	20200	11900	1820	24.5	20	199.65
68-13-406	86300	17900	4980	1890	8.52	8.59	272.2

Table 5.1. Data used to build the Piper plot reported by Corpus Christi Lab. Total Alkalinity as CaCO₃ was taken from the field shield reported by the Edwards Aquifer Authority.

The total alkalinity must be converted from units of mg/L as CaCO₃ to units of meq/L as HCO₃+CO₃ for use in the Piper diagram. With a pH ranging between 7-8 for the waters sampled, CO₃ is not detected. Essentially, all alkalinity is HCO₃ in the samples. Total alkalinity as CaCO₃ was converted to total alkalinity as HCO₃ considering (1) the molecular weight of CaCO₃ = 100g/mol (2) the molecular weight of HCO₃ = 61g/mol and the milliequivalents (meq) per mol of (3) CaCO₃ = 2 and (4) HCO₃ = 1

$$\text{Alkalinity as HCO}_3 \frac{\text{mg}}{\text{L}} =$$

$$\text{Alkalinity as CaCO}_3 \frac{\text{mg}}{\text{L}} \times \frac{1 \text{ mmol CaCO}_3}{100 \text{ mg}} \times \frac{2 \text{ meq}}{1 \text{ mmol CaCO}_3} \times \frac{1 \text{ mmol HCO}_3}{1 \text{ meq}} \times \frac{61 \text{ mg HCO}_3}{1 \text{ mmol HCO}_3}$$

An Equivalent (equals to 1000 milliequivalents (meq)) is defined as the amount of a substance needed to react with one mole of electrons in a reaction. The Piper diagram is built in terms of milliequivalent percentages (meq%). Concentrations in mg/L can be converted to meq/L using the following equation. Values for valences and atomic weights are presented in table 5.2

$$\text{Ion concentration } \left(\frac{\text{meq}}{\text{L}}\right) = \frac{\text{ion concentration } \left(\frac{\text{mg}}{\text{L}}\right) * \text{Valence}}{\text{Atomic weight}} \quad [3]$$

	Cations				Anions		
	Ca	Mg	Na	K	Cl	SO ₄	HCO ₃
Valence	2	2	1	1	1	2	1
Atomic weight	40.07	24.30	22.99	39.09	35.45	96.05	61.0

Table 5.2. Values of Valence and Atomic weight used to calculate ion concentrations in meq/L

Results are presented in table 5.3. This conversion accounts for the valance or ionic charge of each primary ion in the sample.

Site ID	SO ₄ (meq/L)	Cl (meq/L)	Ca (meq/L)	Na (meq/L)	Mg (meq/L)	K (meq/L)	HCO ₃ (meq/L)
68-13-102	0.56	0.40	4.24	0.26	1.25	0.21	5.33
68-05-705	0.42	0.69	2.84	0.54	1.75	0.05	4.04
68-12-302	4.21	8.41	2.07	9.31	2.95	0.31	5.34
68-13-103	0.15	0.38	5.89	0.30	0.67	0.03	6.17
68-13-105	0.25	0.51	5.44	0.37	1.02	0.03	5.94
68-05-704	1.22	1.84	4.34	2.57	3.00	0.17	6.91
68-05-807	4.85	9.68	3.02	10.70	3.80	0.37	5.24
68-13-107	5.23	10.16	2.67	12.01	3.70	0.38	4.76
68-13-210	0.42	0.69	2.73	0.52	1.66	0.05	3.99
68-13-406	0.18	0.24	4.31	0.22	1.47	0.05	5.44

Table 5.3. Ion concentrations in meq/L

The Piper diagram requires the data to be normalized to percent of the total ions. The percentage for each ion is calculated relative to the total cations or anions using the equation [4]. Results are presented in table 5.4.

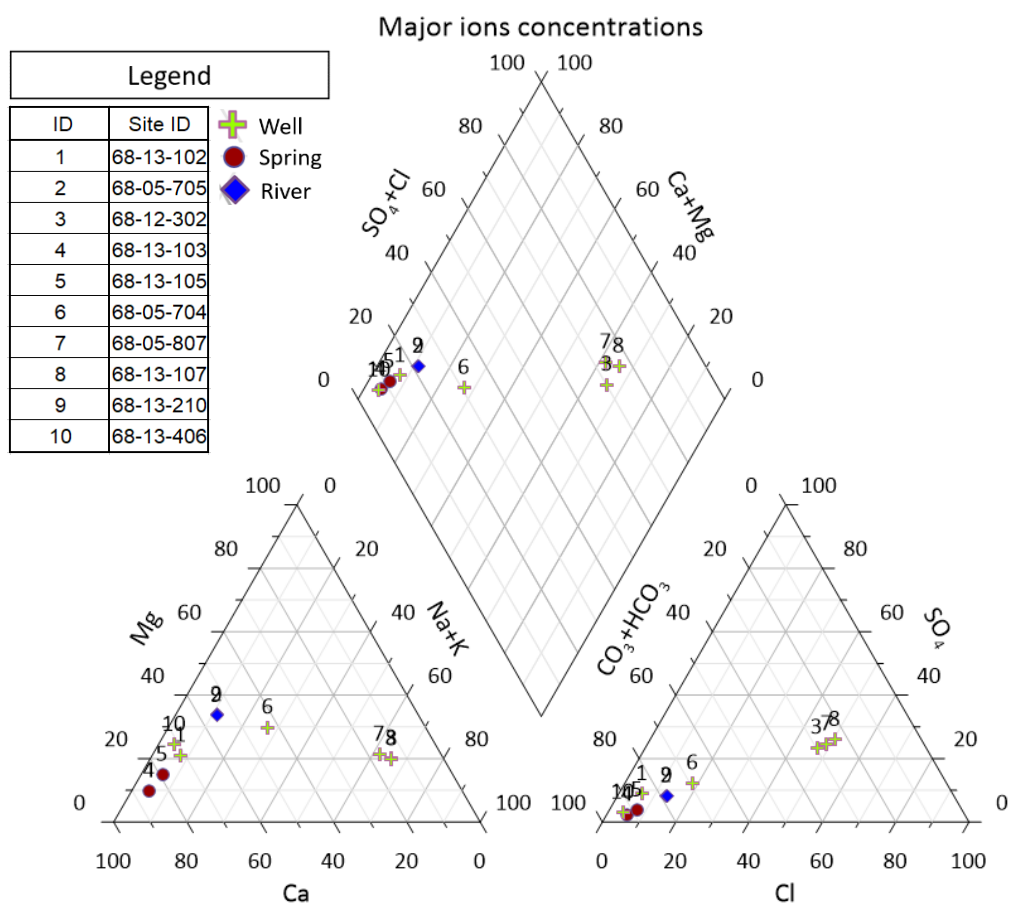
$$\text{Ions concentrations normalized (meq\%)} = \frac{\text{ion concentration (meq/L)} * 100\%}{\text{Total ions (cations or anions) concentrations}}$$

Site ID	Total cations (meq/L)	Total Anions (meq/L)	Ca (meq%)	Mg (meq%)	Na (meq%)	K (meq%)	Cl (meq%)	SO ₄ (meq%)	HCO ₃ (meq%)
68-13-102	5.96	6.29	71.12	21.00	4.31	3.58	6.42	8.84	84.74
68-05-705	5.18	5.16	54.90	33.83	10.33	0.94	13.40	8.24	78.37
68-12-302	14.63	17.95	14.12	20.14	63.63	2.12	46.83	23.43	29.73

68-13-103	6.90	6.70	85.39	9.77	4.42	0.42	5.72	2.28	92.00
68-13-105	6.86	6.69	79.29	14.87	5.40	0.44	7.63	3.67	88.70
68-05-704	10.08	9.98	43.01	29.79	25.50	1.71	18.46	12.27	69.27
68-05-807	17.89	19.77	16.90	21.25	59.81	2.04	48.94	24.54	26.52
68-13-107	18.75	20.14	14.24	19.74	64.01	2.00	50.42	25.95	23.63
68-13-210	4.96	5.10	55.08	33.54	10.44	0.94	13.55	8.17	78.28
68-13-406	6.04	5.86	71.25	24.37	3.58	0.80	4.10	3.05	92.85

Table 5.4 Ion concentrations normalized to the total ions' concentration.

The Piper diagram presented in Figure 5.7 was generated in the software Grapher, using the data from table 5.5.



RESULTS

MAJOR IONS

Most samples can be classified as Ca-HCO₃-Mg type (figure 5.10), which is not surprising, considering that the predominant lithologies in the area are carbonates. Only three wells (68-12-302, 68-05-807, 68-13-107) from the ten sampled sites are classified as Na+Ca-Cl-SO₄-HCO₃ (figure 5.10) and one well (68-05-704) is mixed or Ca-Mg-Na-HCO₃-Cl. Based on the anion content, most of the samples are classified as *bicarbonate type*, with high meq% of HCO₃ (figure 5.10). Wells 68-12-302, 68-05-807, 68-13-107 also present a different chemical classification based on their anion's content *mixed-Chloride type* (Figure 5.8)

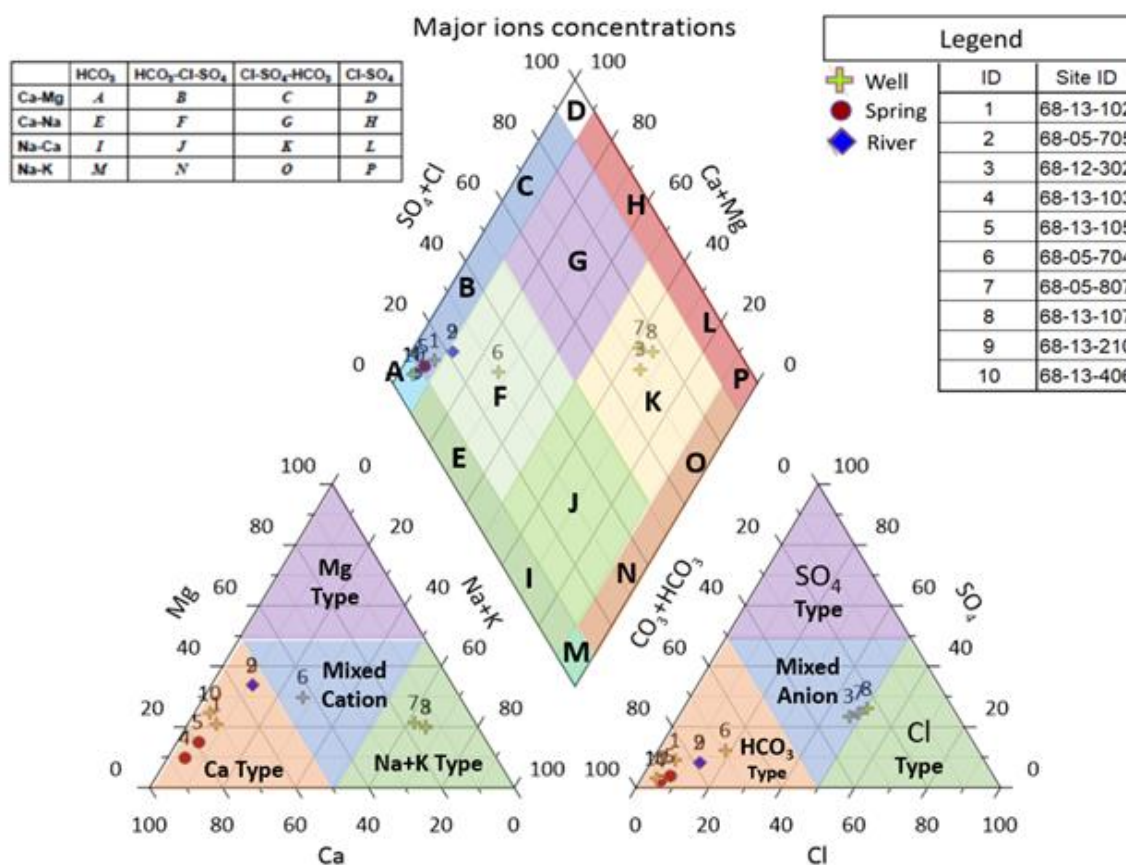


Figure 5.8. Water type based on major ions classification, using the Piper diagram.

NUTRIENTS

The only significant nutrient concentration for all ten samples sites was for nitrate. Two spring sites had the highest concentration of nitrate while two sites on the Guadalupe river had the lowest (Figure 5.11). Ammonia was present for the public supply well (68-12-302) and a private use well (68-13-107). Phosphorus was present only in samples from one well (68-13-102). Total Kjeldahl Nitrogen was present in three well sites (68-13-102; 68-12-302; 68-13-107) and one river

site (68-05-705). Dissolved orthophosphate and nitrite were in concentrations below the lab's detection limit for all ten sites.

Nitrate Concentration

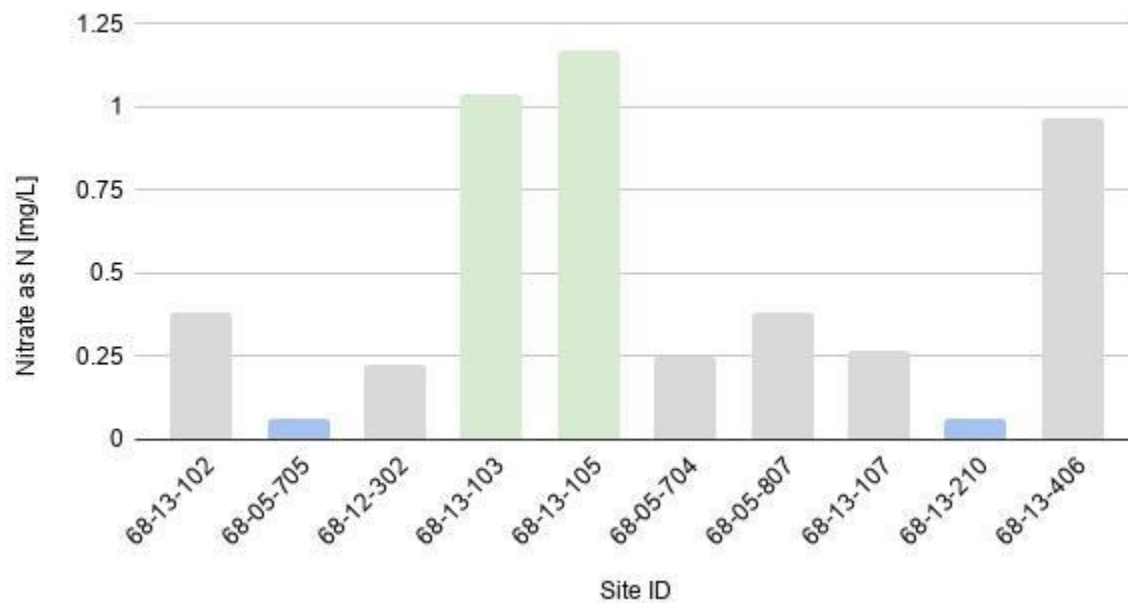


Figure 5.9. The nitrate as N concentration across all ten sites. Gray represents well sites, green represents spring sites, and blue represents sites on the Guadalupe River.

ISOTOPES

Deuterium and oxygen-18 isotope data for all ten samples is shown in Figure 5.10. The data shown are per mil enrichments of the isotopic ratios D/H and O^{18}/O^{16} relative to Vienna Standard Mean Ocean Water (VSMOW). Samples from the well sites and spring sites follow the Global Meteoric Water Line (GMWL). Samples from the river sites deviate from the GMWL and show that kinetic fractionation from evaporation is occurring in the Guadalupe River.

Hydrogen and Oxygen Isotopes

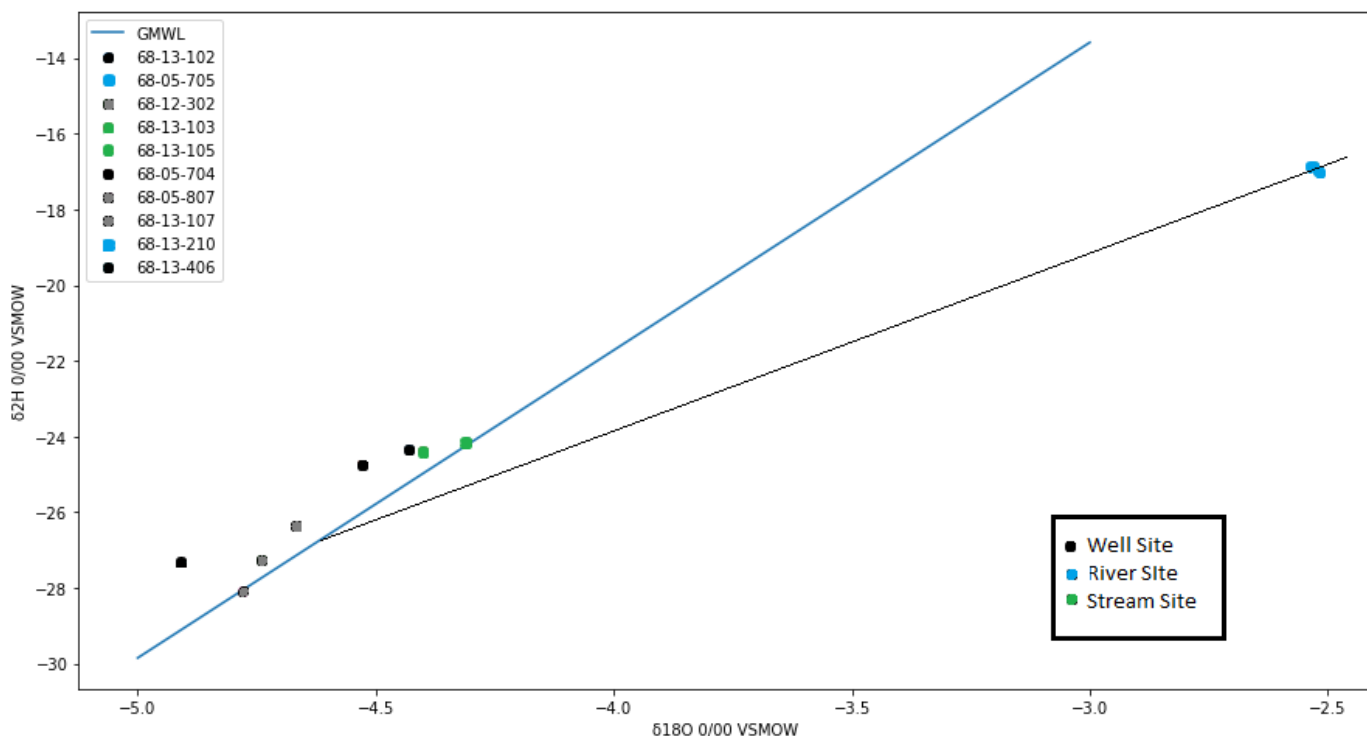


Figure 5.10. D/H and O^{18}/O^{16} across all ten sites. Gray represents Lower Trinity well sites, black represents Middle Trinity well sites, green represents spring sites, and blue represents sites on the Guadalupe River. The black line represents the linear deviation of the river sites due to evaporation.

Percent modern carbon (pMC) and carbon-14 in dissolved inorganic carbon (DIC) data are shown in Figure 5.11. Samples from the Honey Creek spring sites and the Guadalupe river sites had the highest values of pMC. These sites were all above above 75 pMC. Well samples from the Middle Trinity varied between 56 pMC and 85 pMC. Well samples from the Lower Trinity had the lowest values of pMC. These sites were all lower than 25 pMC.

Carbon Isotopes

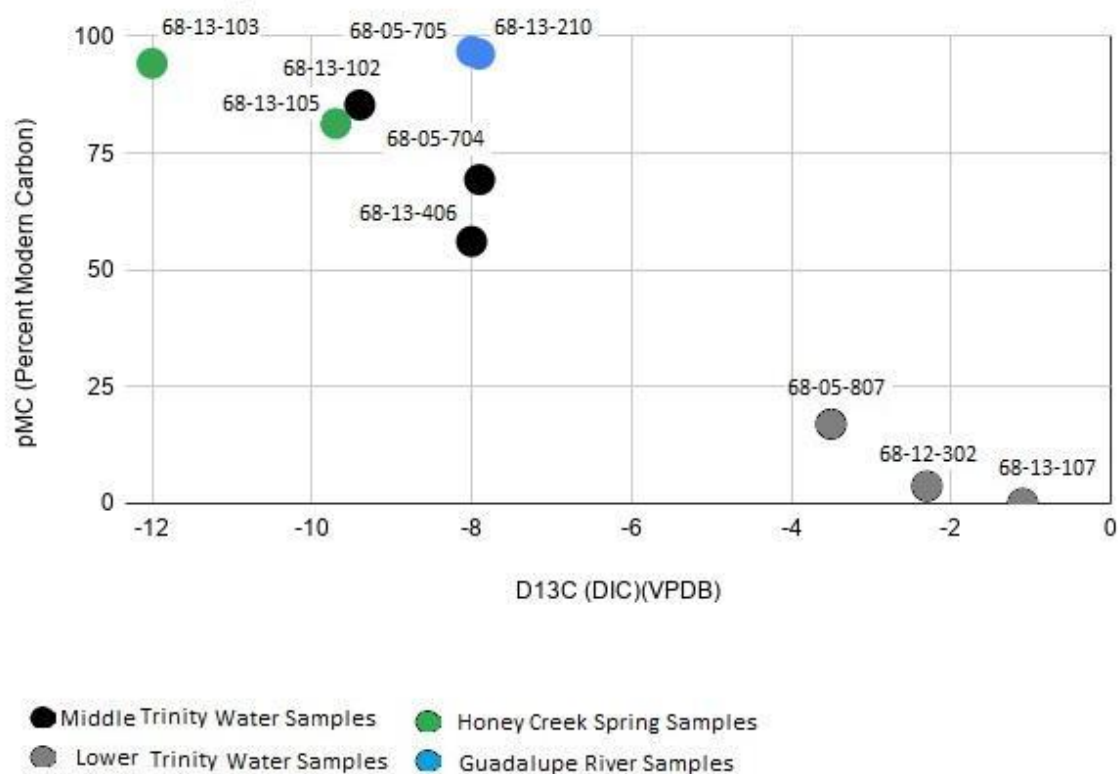


Figure 5.11. pMC and D13C across all ten sites. Gray represents well sites in the Lower Trinity, black represents well sites in the Middle Trinity, green represents spring sites, and blue represents sites on the Guadalupe River.

PFAAS and PPCP

There were 16 categories of Per- and polyfluoroalkyl substances (PFAs) tested in this study. The chemicals include Perfluorobutanoic acid (PFBA), Perfluoropentanoic acid (PFPeA), Perfluorohexanoic acid (PFHxA), Perfluoroheptanoic acid (PFHpA), Perfluorooctanoic acid (PFOA), Perfluorononanoic acid (PFNA), Perfluorodecanoic acid (PFDA), Perfluoroundecanoic acid (PFUnA), Perfluorododecanoic acid (PFDoA), Perfluorotridecanoic acid (PFTriA), Perfluorotetradecanoic acid (PFTeA), Perfluorobutanesulfonic acid (PFBS), Perfluorohexanesulfonic acid (PFHxS), Perfluorooctanesulfonic acid (PFOS), Perfluorodecanesulfonic acid (PFDS), and Perfluorooctanesulfonamide (PFOSA).

The chemical analysis in this study found that out of the 16 categories of PFASs, only 1 of the tested substances was undisputedly detected in the lab. The chart below (Table 5.5) shows the results for the chemical analysis for all the sites, and the key to the data detection likelihood.

Site ID	Classification	PFBA	PFPeA	PFHxA	PFHpA	PFOA	PFNA	PFDA	PFUnA
68-13-102	Well	2.71							
68-05-705	River	1.27	0.757	0.636	0.305	0.905			
68-12-302	Well								
68-13-103	Spring								
68-13-105	Spring								
68-05-704	Well								
68-05-807	Well								
68-13-107	Well								
68-13-210	River	1.16	0.559	0.796	0.259	0.829			
68-13-406	Well								
Site ID	Classification	PFDoA	PFTriA	PFTeA	PFBS	PFHxS	PFOS	PFDS	PFOSA
68-13-102	Well								0.328
68-05-705	River				0.978				
68-12-302	Well								
68-13-103	Spring								
68-13-105	Spring				0.218				
68-05-704	Well								
68-05-807	Well								
68-13-107	Well								
68-13-210	River				0.764				0.412
68-13-406	Well								
KEY									
#	Value reported above RL (real detection)								
#	Value below RL, above MDL, value greater than 50% of MDL, value greater than 1/2 RL (likely detection)								
#	Value below RL, above MDL, value greater than 50% of MDL, value less than 1/2 RL (possible detection)								
#	Value below RL, above MDL, value less than 50% of MDL, valueless than 1/2 RL (questionable detection)								
	Sample below RL, above and/or below MDL, analyte detected in blank (no detection)								

Table 5.5. The results of the lab PFAS analysis for all the sites and key.

Many of the lab reported PFAS values are below the reporting limit and found the tested chemical in their blanks, so those values were not reported. The samples that were below the reporting limit but above the minimum detection limit and did not find the tested chemicals in the blanks were reported in the key above. The minimum detection limits for all the PFASs are shown below. Although some of the samples were above the minimum detection limit, only one site sample was also above the reporting limit.

The river PFAS results from the tests are graphed below, since these had the most consistent detections of the chemicals compared to the other sites.

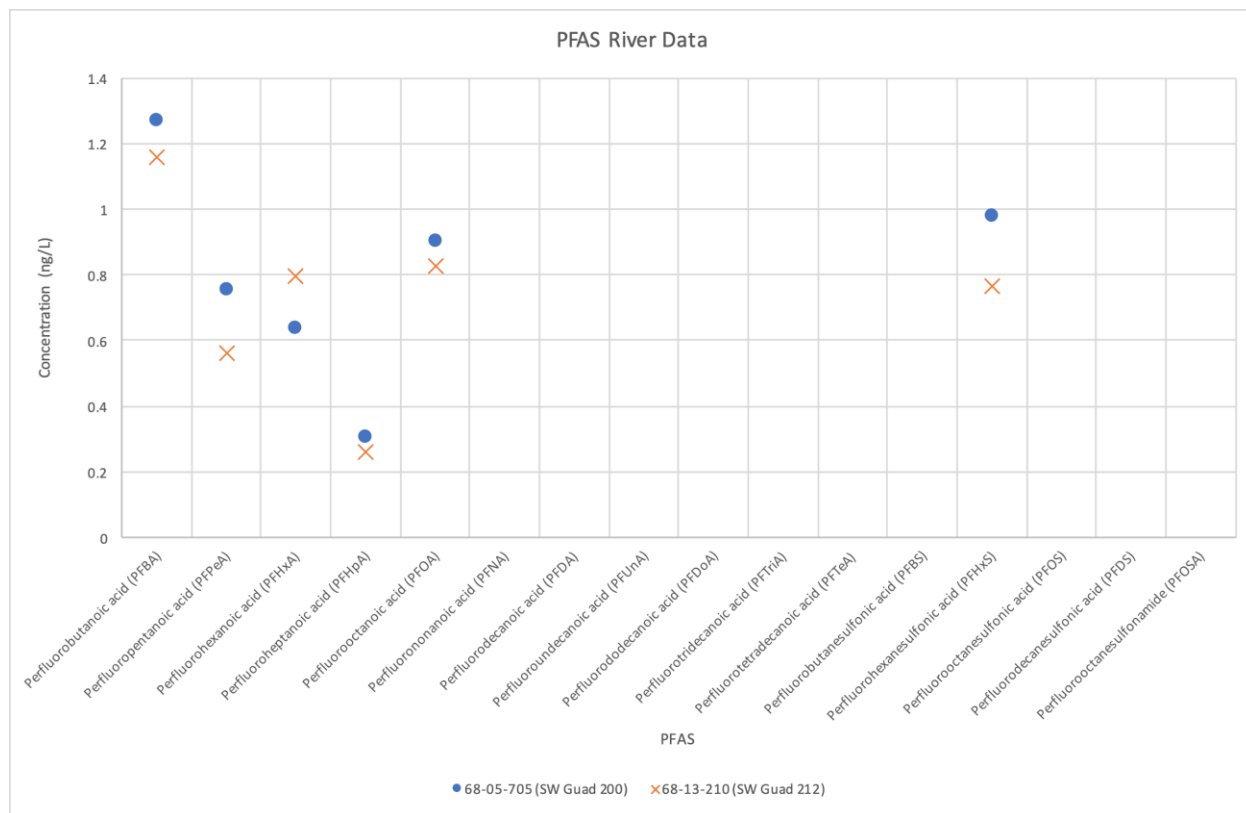


Figure 5.12. The concentration of the PFASs at all the river sites. These sites include 68-05-705 and 68-13-210.

The sites were also tested for a range of personal care products and pharmaceuticals (PCPPs), but the concentrations for all the tested sites have not been received from the lab yet. The table below shows all the PCPPs that the water samples were tested for.

Pharmaceuticals and Personal Care Products Tested				
Acetaminophen	Diclofenac	Fluoxetine	Hydrocodone	Insulin
Aspirin	Diclofenac	Fluoxetine	Hydrocodone	3 Insulin
Chlorzoxazone	Diclofenac	Fluoxetine	Hydrocodone	
Clozapine	Diclofenac	Fluoxetine	Hydrocodone	
Cyclosporine	Diclofenac	Fluoxetine	Hydrocodone	
Diazepam	Diclofenac	Fluoxetine	Hydrocodone	
Doxycycline	Diclofenac	Fluoxetine	Hydrocodone	
Ethinylloestradiol	Diclofenac	Fluoxetine	Hydrocodone	
Fluoxetine	Diclofenac	Fluoxetine	Hydrocodone	
Hydrocodone	Diclofenac	Fluoxetine	Hydrocodone	

□ □ □ □ □ □ □ □ □ □	□ □ □ □ □ □ □ □	R □ □ □ □ □ □ □ □ □ □	□ □ □ □ □ □ □ □ □ □	
□ □ □ □ □ □ □ □	□ □ □ □ □ □ □ □ □ □	□ □ □ □ □ □ □ □ □ □	□ □ □ □ □ □ □ □ □ □	
D □ □ □ □ □ □ □ □ □ □	M □ □ □ □ □ □ □ □	□ □ □ □ □ □ □ □ □ □ □ □ □ □	□ □ □ □ □ □ □ □	

Table 5.6. The PCPPs tested for in the water samples.

DISCUSSION

MAJOR IONS

The major ion composition of the samples is highly controlled by the lithology of the region. Samples collected in wells, rivers, and springs present a high concentration of Ca and bicarbonate (figure 5.8) , which is explained by a lithology dominated by carbonates.

Sample 68-05-705 and 68-13-210 were collected in the Guadalupe River upstream and downstream from a residential area (Figure 5.12). These samples present almost indistinguishable major ions concentrations dominated by Ca and HCO₃. Samples collected in springs (68-13-103 and 68-13-105) present higher concentrations of Ca and HCO₃, than those taken in the river. Springs are sites where groundwater flow reaches surface; it is expected that the water samples from these sites have a signature closer to the groundwater samples in comparison with the samples collected in the river (more diluted and contaminated with other elements).

Finally, we sampled six wells. Three of them completed in the Middle Trinity Aquifer (68-13-102, 68-05-704 and 68-13-406) and three completed in the Lower Trinity Aquifer (68-12-302, 68-05-807 and 68-13-107). Once more, lithology seems to dominate major ions in the sampled sites. Wells completed in the Lower Trinity Aquifer present higher concentrations of Cl, sulfate, Na and K, while wells completed in the Middle Trinity Aquifer present higher concentrations of Ca and bicarbonate. Well 68-05-704 is a deep well (315 ft). The surface geology in the well location corresponds to Honey creek considering the thickness of the underlying formations, Honey creek= 55ft, Hensel= 50ft, Cow creek =70ft and Hammett= 30ft (Clark, *et al.* 2016) this well would be completed in the Lower Trinity aquifer, going beyond of the Hammett formation (confining unit). As shown in figure 5.10 this well presents a mixed chemical signature, which could be explained by a mix of waters from the Lower and Middle Trinity aquifers.

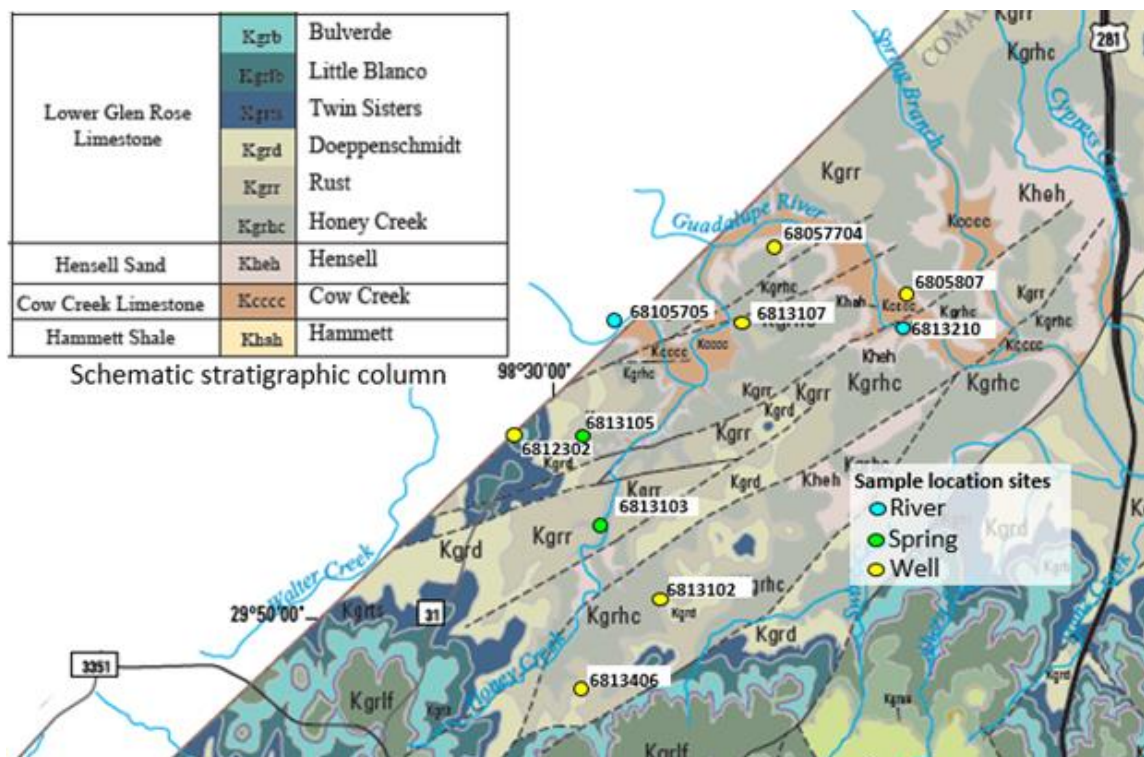


Figure 5.13. Geologic map and schematic stratigraphic column in the study area.

NUTRIENTS

The nitrate concentration for the wells and the Guadalupe River either match or are below what would be expected for water without an external source for nutrient compounds. National background concentrations of nitrate have been estimated to be 0.24 mg/L for streams and 1.0 mg/L for groundwater (Dubrovsky et al, 2010). The nitrate concentration for the sites on the Guadalupe River and the well sites are below the national background for water in the United States. At 1.04 mg/L and 1.17 mg/L, the nitrate concentration for the spring sites are slightly higher than the national background.

The concentrations for nitrate and nitrite were below the maximum contaminant level (MCL) for drinking water established by the U.S. Environmental Protection Agency. For nitrate, it is 10 mg/L and for nitrite it is 1 mg/L (U.S. Environmental Protection Agency, 2019).

Since phosphorus concentration was very low for all sample sites, excess algae growth at the selected sites is not a concern at this time. Phosphorus availability is a critical factor controlling eutrophication as it is frequently the nutrient in most limited supply in aquatic systems (Hem, 1992).

The source for the higher nitrate concentration on the spring samples and well 68-13-406 is unknown. Potential sources include fertilizers, human and animal waste, septic system drainage, runoff from lawns, and precipitation (Mahler et al., 2011).

ISOTOPES

D/H and O18/O16 in samples from the well sites and spring sites plot along the GMWL. This indicates that there is a meteoric water source and that evaporation is not occurring in significant amounts during recharge. Samples from the river sites deviate from the GMWL and show that kinetic fractionation from evaporation is occurring in the Guadalupe River.

Samples from the Honey Creek spring sites and the Guadalupe river sites had the highest values of pMC. Well samples from the Lower Trinity had the lowest values of pMC. It is currently unknown as to whether these differences in pMC are due to a difference in water source, a function of recharge dynamics, a result of atmosphere exchange, or some combination of all three. It would be expected for the river sites to have relatively young water since water is constantly being cycled through it. It is possible that there is limited interaction and flow paths between the Middle Trinity and the Lower Trinity as made evident by difference in the relative ages of their water samples. More sampling in this area is needed to fully understand the flow paths and recharge sources for the Middle and Lower Trinity aquifer, the Guadalupe River, and springs around Honey Creek.

PFAS and PPCP

Overall, the numbers of PFAS detected in the tested sites were very low. Out of 16 tested compounds, only 1 was confidently detected by the lab.

The river test sites (68-05-705 and 68-13-210) had the maximum amount of detections, while the springs and wells only had one questionable PFAS detection. The only 'real detection' was Perfluorobutanoic acid (PFBA) in the State Natural Area Water Well (68-13-102), which is used in fluoropolymers such as teflon. The general trend shows that the upstream river site (68-05-705) had either somewhat higher or equal concentrations of PFAS than the downstream site (68-13-210). Only in the Perfluorohexanoic acid (PFHxA) detection did the downstream site have a larger PFAS value. Perfluorohexanoic acid (PFHxA) is used to create fluorinated polymers, which are materials that have a high chemical resistance and low friction coefficient.

CONCLUSION

The major ion composition of the samples is highly controlled by the lithology of the region. Samples collected in wells, rivers and springs present a high concentration of Ca and bicarbonate (figure 5.10), which reflects the dominant lithology of the region, carbonates. Samples collected in the river present almost indistinguishable major ions concentrations dominated by Ca and HCO₃. Samples collected in springs present higher concentrations of Ca and HCO₃ than those taken in the river. Waters from wells completed in the Lower Trinity Aquifer present higher concentrations of Cl, sulfate, Na and K, while wells completed in the Middle Trinity Aquifer present higher concentrations of Ca and bicarbonate. Well 68-05-704 presents a mixed chemical signature, which could be explained by a mix of waters from the Lower and Middle Trinity aquifers.

Nutrient concentration was very low for all sites tested with nitrate being the only nutrient species to show up in every site sample. It was relatively high for the spring sites and relatively low for the river sites tested.-

D/H and O18/O16 isotope data show a meteoric source for the well and spring sample sites with very little evaporation occurring during recharge. Samples from the river sites show that kinetic fractionation from evaporation is occurring in the Guadalupe River.

Most of the water was relatively young with pMC values being above 50 percent. The exception to this were well sites from the Lower Trinity. For these sample, the pMC was below 25 percent.

The amount of PFAS in the tested waters were very small, with only one of the chemicals were indisputably detected. The general trend in the river sites was that the upstream had either the same or a somewhat higher concentration of PFAS than the downstream sites, but since there were only two samples taken there is no definite trend.

CHAPTER 6 – Conclusion

In the ever-evolving populace and landscape of the hill country area in Central Texas, the need for both potable water supplies and wastewater treatment solutions will continue to expand. This is a region that relies chiefly on groundwater from the Edwards and Trinity Aquifers to supply potable water to over 2 million people and to also provide for municipal and industrial uses. The complex karst nature of this region, as well as the spatial and temporal variability of groundwater and surface interaction, makes estimates of recharge and contamination risk a difficult task. This report sought to characterize the current conditions within the Guadalupe River basin and Middle Trinity Aquifer in the vicinity of Honey Creek in western Comal County in order to provide a comparative baseline as pumping, population, and wastewater discharge into the study area increase in the coming years. The report detailed the data collected by the Applied Karst Hydrogeology Fall 2019 course at the University of Texas at Austin, taught by Dr. Marcus Gary. The following findings were made: (1) In terms of the hydrogeologic framework & major features within the study area, a map was generated of Rebecca Cave, the origin of Rebecca Creek. A fault next to the Guadalupe River, hereby named Esser's Fault, was discovered and mapped. (2) In terms of surface water, there was measured groundwater recharge from the Guadalupe River at 7,696 acre-feet over the duration of the study. (3) In terms of groundwater, an overall regional trend of groundwater flow from northwest to southeast in the Middle Trinity Aquifer was observed. (4) In terms of water chemistry, there were low nutrient concentrations at all sites. Spring sites had elevated nitrate compared to river sites. The PPCP lab results have not arrived at the time of this reports publication. Finally, there were almost no PFAs detections. From these findings and additional findings, the major conclusions of this study were that this region has surface water-groundwater connectivity, especially due to the large karst features such as Honey Creek Cave, and that the major ion concentrations in the water samples are highly controlled by the dominant lithology, with the Lower Trinity Aquifer having high concentrations of chlorine, sulfate, sodium, and potassium, and the surface water having high concentrations of calcium and bicarbonate. These results provided a characterization of the Honey Creek study area during a time period of Fall 2019 and with hope, will be utilized for future studies and hydrogeological characterizations of the hill country and Central Texas region.

Chapter 7-References

- About the Texas Water Development Board Texas Water Development Board,
<http://www.twdb.texas.gov/about/index.asp> (accessed December 2019).
- Bakalowicz, M., 2005, Karst groundwater, A challenge for new resources: *Hydrogeology Journal*, v. 13, p. 148–160, doi:10.1007/s10040-004-0402-9.
- Barker, R.A., and Ardis, A.F., 1996, Hydrogeologic framework of the Edwards-Trinity aquifer system, west-central Texas:, doi:10.3133/pp1421b.
- Barker, R.A., Bush, P.W., and Baker, E.T., Jr., 1994, Geologic History and Hydrogeologic Setting of Edwards-Trinity Aquifer System, West-Central Texas: U.S. Geological Survey Water Resources Investigations Report 94-4039, 55 p.
- Brendel, S., Fetter, É., Staude, C., Vierke, L., and Biegel-Engler, A., 2018, Short-chain perfluoroalkyl acids: environmental concerns and a regulatory strategy under REACH: *Environmental Sciences Europe*, v. 30, doi: 10.1186/s12302-018-0134-4.
- Brune, G., 1975. Major and Historical Springs of Texas, Texas Water Development Board Report 189.https://www.twdb.texas.gov/publications/reports/numbered_reports/doc/R189/R189.pdf.
- Brune, G., 1981. Springs of Texas, Volume 1. A&M University agriculture series no. 5.
- Calvin, A. E. Jr., and Quinlan J. F., 1996, Introduction to practical techniques for tracing groundwater in carbonates and other fractured rocks. In *Guidelines for Wellhead and Springhead Protection Area Delineation in Carbonate Rocks*, G.M. Schindel, J.F. Quinlan, G.J. Davies, and J.A. Ray, US EPA Region IV Groundwater Protection Branch, 195 pp.
- Chadha, D. K., 1999, A proposed new diagram for geochemical classification of natural waters and interpretation of chemical data. *Hydrogeology Journal* (Vol. 7). Springer-Verlag.
- Clark, A.K., 2003, Geologic Framework and Hydrogeologic Characteristics of the Edwards Aquifer, Uvalde County, Texas: Water Resources Investigations Report 03-4010, 23 p.
- Clark, A.K., Golab, J.A., and Morris, R.R., 2016, Geologic Framework and Hydrostratigraphy of the Edwards and Trinity Aquifers Within Northern Bexar and Comal Counties, Texas: U.S. Geological Survey, 1–20 p.
- Clark, A.K., Golab, J.A., and Morris, R.R., 2016, Geologic framework and hydrostratigraphy of the Edwards and Trinity aquifers within northern Bexar and Comal Counties, Texas: U.S. Geological Survey Scientific Investigations Map 3366, 1 sheet, scale 1:24,000, pamphlet, <https://doi.org/10.3133/sim3366>.

- Craig, H., 1961, Isotopic Variations in Meteoric Waters: *Science*, v. 133, p. 1702–1703, doi: 10.1126/science.133.3465.1702.
- Drought in Texas, 2019, Drought.gov U.S. Drought Portal, <https://www.drought.gov/drought/states/texas> (accessed November 2019).
- Drought in Texas, 2019, Texas | Drought.gov, <https://www.drought.gov/drought/states/texas> (accessed November 2019).
- Drought in Texas Water Data For Texas, <https://www.waterdatafortexas.org/drought> (accessed November 2019).
- Environmental Protection Agency, 2018, “Basic Information on PFAS”: www.epa.gov/pfas/basic-information-pfas#tab-1 (accessed November 2019).
- Fahlquist, B.L., Ardis, A.F., and Norton, G.A., Survey, U.S.G., 2004, Quality of Water in the Trinity and Edwards Aquifers, South-Central Texas, 1996 – 98 Scientific Investigations Report 2004 – 5201 U . S . Department of the Interior: Quality,.
- Gams, I., 1993, Origin of the term “karst,” and the transformation of the classical karst (kras): *Environmental Geology*, v. 21, p. 110–114, doi:10.1007/BF00775293.
- Gary, M., Rucker, D., Smith, B., Smith, D., and Befus, K., 2017, Geophysical Investigations of the Edwards-Trinity Aquifer System at Multiple Scales: Interpreting Airborne and Direct-Current Resistivity in Karst: , p. 195–206, doi:10.5038/9780979542275.1127.
- Gillon, M., Barbecot, F., Gibert, E., Alvarado, J.C., Marlin, C., and Massault, M., 2009, Open to closed system transition traced through the TDIC isotopic signature at the aquifer recharge stage, implications for groundwater 14C dating: *Geochimica et Cosmochimica Acta*, v. 73, p. 6488–6501, doi: 10.1016/j.gca.2009.07.032.
- Groundwater Conservation District and Groundwater Management Plan FAQs FAQs - Groundwater Conservation Districts | Texas Water Development Board, <http://www.twdb.texas.gov/groundwater/faq/index.asp#title-01> (accessed November 2019).
- Groundwater Data Texas Water Development Board, <http://www.twdb.texas.gov/groundwater/data/index.asp> (accessed November 2019).
- Hill Country Alliance, 2008, Growth of the Hill Country: Following the path we are on today through 2030, Pegasus Planning.
- Hunt, B.B., Smith, B.A., Gary, M., Broun, A.S., Wierman, D.A., Watson, J., and Johns, D., 2017, Surface-water and groundwater interactions in the Blanco River and Onion Creek watersheds: Implications for the Trinity and Edwards Aquifers of central Texas: *South Texas Geological Society*, v. 57, p. 53, doi:10.5038/9780991000982.1044.

- Jie, C., Hanting, Z., Hui, Q., Jianhua, W., and Xuedi, Z., 2013, Selecting Proper Method for Groundwater Interpolation Based on Spatial Correlation: 2013 Fourth International Conference on Digital Manufacturing & Automation, p. 1–5, doi: 10.1109/icdma.2013.282.
- Jones, I.C., Anaya, R., and Wade, S.C., 2011, Groundwater Availability Model: Hill Country Portion of the Trinity Aquifer of Texas: Texas Water Development Board.
- Jones, I.C., Anyaya, R., Wade, S.C., 2011. TWDB, 2011. Groundwater Availability Model: Hill Country Portion of the Trinity Aquifer of Texas. TWDB Report 377.
- Klimchouk, A.B., 2016, The Karst Paradigm: Changes, Trends and Perspectives: *Acta Carsologica*, v. 44, p. 289–313, doi:10.3986/ac.v44i3.2996.
- Mabe, J.A., 2007, Nutrient and biological conditions of selected small streams in the Edwards Plateau, Central Texas, 2005–06, and implications for development of nutrient criteria: U.S. Geological Survey Scientific Investigations Report 2007–5195, 46 p.
- Mace, R.E., Chowdhury, A.H., Anaya, R., and Way, S.-C., 2000, Groundwater Availability of the Trinity Aquifer, Hill Country Area, Texas: Numerical Simulations through 2050: Texas Water Development Board, 1–112 p.
- Mahler, B.J., Musgrove, M., Herrington, C., and Sample, T.L., 2011, Recent (2008–10) concentrations and isotopic compositions of nitrate and concentrations of wastewater compounds in the Barton Springs zone, south-central Texas, and their potential relation to urban development in the contributing zone: U.S. Geological Survey Scientific Investigations Report 2011–5018, 39 p.
- Mahler, B.J., Musgrove, M., Sample, T.L., and Wong, C.I., 2011, Recent (2008–10) water quality in the Barton Springs segment of the Edwards aquifer and its contributing zone, central Texas, with emphasis on factors affecting nutrients and bacteria: U.S. Geological Survey Scientific Investigations Report 2011–5139, 66 p.
- Martin, N., Green, R., Nicholaidis, K., Fratesi, S.B., Nunu, R., and Flores, M., 2019, Blanco River Aquifer Assessment Tool A Tool to Assess How the Blanco River Interacts with Its Aquifers : Creating the Conceptual Model.
- Menking, K., 2019, Map of Honey Creek Cave Entrance Passage.
- Menking, K., 2019, Private Lecture.
- Palmer, A. N., 1991, Origin and morphology of limestone caves: *GSA Bulletin*; 103 (1): 1–21.
- San Antonio, Texas Population 2019, 2019, San Antonio, Texas Population 2019 (Demographics, Maps, Graphs), <http://worldpopulationreview.com/us-cities/san-antonio-population/> (accessed December 2019).

Saribudak, M., 2016. Geophysical mapping of Mount Bonnell fault of Balcones Fault zone and its implications on Trinity-Edwards Aquifer interconnection, central Texas, USA. *The Leading Edge* 35(9). September 2016.

Sharp, J.M., and Banner, J.L., 1997, *The Edwards Aquifer: A Resource in Conflict*: GSA Today, v. 7, p. 1–8.

Sidle, W. C., 1997, *Environmental Isotopes for Resolution of Hydrology Problems*, U.S. Environmental Protection Agency, National Risk Management Research Laboratory, 22 p.

The State of Water in the Hill Country Texas Parks and Wildlife,
<https://tpwd.texas.gov/landwater/water/environconcerns/regions/hillcountry.phtml>
(accessed December 2019).

Toll, N.J., Green, R.T., McGinnis, R.N., Stepchinski, L.M., Nunu, R.R., Walter, G.R., Harding, J., Deeds, N.E., Flores, M.E., and Gulliver, K.D.H., 2018, *Conceptual Model Report for the Hill Country Trinity Aquifer Groundwater Availability Model* : Texas Water Development Board , 1–121 p.

Veni, G., 1997, “Geomorphology, hydrogeology, geochemistry, and evolution of the karstic Lower Glen Rose Aquifer, South-Central Texas.”. Ph.D. dissertation, Pennsylvania State University. *Texas Speleological Survey Monographs*, 1, p 409.

Water Data for Texas, 2019
<https://www2.twdb.texas.gov/apps/waterdatainteractive/groundwaterdataviewer>
(accessed 2019).

White, W.B., 2002, *Karst hydrology: Recent developments and open questions*: *Engineering Geology*, v. 65, p. 85–105, doi:10.1016/S0013-7952(01)00116-8.

White, W. B., 2002, “Karst Hydrology: Recent Developments and Open Questions.” *Engineering Geology*, vol. 65, no. 2-3, pp. 85–105., doi:10.1016/s0013-7952(01)00116-8.

Yelderman, Joe C., Jr., ed. 1987. *Hydrogeology of the Edwards Aquifer, Northern Balcones and Washita Prairie Segments*. Guidebook 11, Austin Geological Society, 104 pp.

Zara Environmental, Veni and Associates. 2010. *Hydrogeological, biological, archeological, and paleontological karst investigations, Camp Bullis, Texas*. Prepared for Natural and Cultural Resources Environmental Division, Fort Sam Houston, San Antonio, Texas.

Zara Environmental. 2011. *Karst hydrogeology of Camp Bullis, Bexar and Comal Counties: A window into the Edwards-Trinity aquifer system*. Prepared for Natural and Cultural Resources Environmental Division, Fort Sam Houston, San Antonio, Texas.